Gazi Üniversitesi
Fen Bilimleri Dergisi
PART C: TASARIM VE TEKNOLOJİ

Gazi University
Journal of Science
PART C: DESIGN AND TECHNOLOGY

GU J Sci, Part C, 14(3): 1258-1279 (2026)

Effect of Bentonite Replacement and Polypropylene Fiber Reinforcement on Physico-Mechanical and Durability Performance of One-Part Slag-Based Geopolymer Foam Concretes

Oğuzhan Yavuz BAYRAKTAR[1] Gökhan KAPLAN[2*]

[1]*Kastamonu University, Faculty of Engineering and Architecture, Department of Civil Engineering, Kastamonu, Tirkiye*

[2*]*Atatürk University, Faculty of Engineering, Department of Civil Engineering, Erzurum, Tirkiye*

Article Info

Research article
Received: 03/01/2026
Revision: 02/03/2026
Accepted: 11/03/2026

Keywords

Bentonite
Polypropylene fiber
Freeze-thaw effect
Geopolymer foam concrete
Sorptivity

Makale Bilgisi

Araştırma makalesi
Başvuru: 03/01/2026
Düzeltme: 02/03/2026
Kabul: 11/03/2026

Anahtar Kelimeler

Bentonit
Polipropilen lif
Donma-çözülme etkisi
Geopolimer köpük beton
Kapilarite

Graphical/Tabular Abstract (Grafik Özet)

This study investigates the physico-mechanical and durability properties of one-part slag-based geopolymer foam concretes containing bentonite and polypropylene fibers, revealing the foam collapse mechanism caused by excessive rheology from the bentonite-PPF combination. / Bu çalışma, bentonit ve polipropilen lif içeren tek bileşenli cüruf esaslı geopolimer köpük betonların fiziko-mekanik ve dayanıklılık özelliklerini incelemekte; bentonit-PPF kombinasyonunun yüksek reolojiye bağlı köpük çökmesi mekanizmasını ortaya koymaktadır.

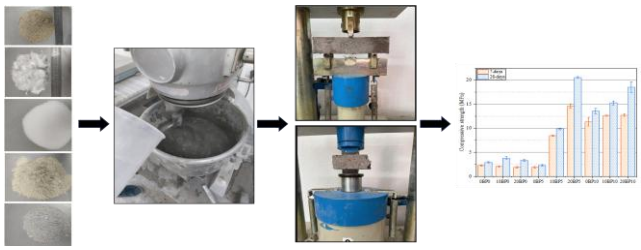

***Figure A**: Production process of GFCs /**Şekil A:** Geopolimer köpük beton numunesi üretim süreci*

Highlights (Önemli noktalar)

- *Bentonite-PPF combination causes foam collapse beyond a critical rheological threshold.*
- *Stable foams provide low density and superior insulation; collapsed mixes provide high strength and freeze-thaw resistance.*
- *Bentonite significantly improves thermal stability at 750°C.*
- *Bentonit-PPF kombinasyonu kritik reolojik eşiği aştığında köpük çökmesine yol açar.*
- *Kararlı köpükler düşük yoğunluk ve üstün yalıtım; çöken karışımlar yüksek dayanım ve donma-çözülme direnci sağlar.*
- *Bentonit 750°C'de termal stabiliteyi önemli ölçüde artırır.*

***Aim (Amaç):** This study investigates the effects of bentonite and PPF on geopolymer foam concrete properties to reveal the critical rheological threshold destabilizing foam and propose design criteria for insulation-strength balance. / Bu çalışma, bentonit ve PPF'nin geopolimer köpük beton özelliklerine etkisini belirleyerek köpük stabilitesini bozan kritik reolojik eşiği ortaya koymak ve yalıtım-dayanım dengesi için tasarım kriterleri önermektedir*

***Originality (Özgünlük):** This study is the first to quantitatively define the foam collapse mechanism caused by bentonite-PPF interaction under excessive yield stress and explain the effect of this rheological transformation on macroscopic properties. / Çalışma, bentonit-PPF etkileşiminin yüksek verim gerilmesine bağlı köpük çökmesi mekanizmasını ilk kez niceliksel olarak tanımlamakta ve bu reolojik dönüşümün makroskopik özellikler üzerindeki etkisini açıklamaktadır.*

***Results (Bulgular):** Foam collapse divided mixes into low-density insulating foams (641 kg/m³, 0.172 W/m·K) and dense high-strength mortars (1779 kg/m³, 20.56 MPa), while bentonite improved thermal stability at 750°C. / Köpük çökmesi, karışımları düşük yoğunluklu yalıtımlı köpük (641 kg/m³, 0,172 W/m·K) ve yoğun yüksek dayanımlı harç (1779 kg/m³, 20,56 MPa) olarak iki gruba ayırmış; bentonit 750°C'de termal stabiliteyi iyileştirmiştir.*

***Conclusion (Sonuç):** Combined use of bentonite and PPF produces lightweight insulating geopolymer composites when rheology is controlled, or high-strength composites otherwise, with 0.5% PPF and <10% bentonite being the optimum limit for stable foam structure. / Bentonit ve PPF'nin birlikte kullanımı reoloji kontrol altında tutulduğunda hafif yalıtımlı, aksi halde yüksek dayanımlı geopolimer kompozitler üretilmesini sağlar ve 0,5% PPF-<%10 bentonit kararlı köpük yapısı için optimum sınırdır.*

*Corresponding author, e-mail: gkaplan@atauni.edu.tr
DOI: 10.29109/gujsc.1855241

GU J Sci, Part C, 14(3): 1258-1279 (2026)

Gazi Üniversitesi
Fen Bilimleri Dergisi
PART C: TASARIM VE TEKNOLOJİ

Gazi University
Journal of Science
PART C: DESIGN AND TECHNOLOGY

http://dergipark.gov.tr/gujsc

Effect of Bentonite Replacement and Polypropylene Fiber Reinforcement on Physico-Mechanical and Durability Performance of One-Part Slag-Based Geopolymer Foam Concretes

Oğuzhan Yavuz BAYRAKTAR[1] Gökhan KAPLAN[2*]

[1]*Kastamonu University, Faculty of Engineering and Architecture, Department of Civil Engineering, Kastamonu, Tirkiye*

[2*]*Atatürk University, Faculty of Engineering, Department of Civil Engineering, Erzurum, Tirkiye*

Article Info

Research article
Received: 03/01/2026
Revision: 02/03/2026
Accepted: 11/03/2026

Keywords

Bentonite
Polypropylene fiber
Freeze-thaw effect
Geopolymer foam concrete
Sorptivity

Abstract

This study examines the physical, mechanical, and durability characteristics of a one-part slag-based geopolymer foam concrete (GFC) that incorporates bentonite (0-20%) and polypropylene fibers (PPF, 0-1%). While the main goal was to achieve a low-density material with good mechanical durability, the combination of bentonite and PPF unexpectedly caused a 'foam collapse' issue. Bentonite's high water absorption and the physical network formed by PPF together increased the paste's yield stress beyond a critical level, leading to foam bubble breakdown during mixing. As a result, the mixes divided into two distinct groups: (1) Stable GFCs (e.g., 0BP5) with low density (641 kg/m³), high porosity (61.2%), and excellent thermal insulation (0.172 W/mK), but low compressive strength (2.32 MPa); and (2) Densified mortars (e.g., 20BP5) with higher density (1779 kg/m³), greater strength (20.56 MPa), and better freeze-thaw resistance (1.84% mass loss), though they lost insulating properties (0.543 W/m.K). Additionally, high-temperature tests showed that bentonite improved thermal stability significantly at 750°C. Ultimately, the findings emphasize that controlling rheology is key to balancing insulation and strength in GFC development.

Bentonit İkamesi ve Polipropilen Lif Takviyesinin Tek Bileşenli Cüruf Esaslı Geopolimer Köpük Betonların Fiziko-Mekanik ve Dayanıklılık Performansı Üzerindeki Etkisi

Makale Bilgisi

Araştırma makalesi
Başvuru: 03/01/2026
Düzeltme: 02/03/2026
Kabul: 11/03/2026

Anahtar Kelimeler

Bentonit
Polipropilen lif
Donma-çözülme etkisi
Geopolimer köpük beton
Kapilarite

Öz

Bu çalışma, bentonit (0-20%) ve polipropilen elyaf (PPF, 0-1%) içeren tek bileşenli cüruf esaslı geopolimer köpük betonun (GFC) fiziksel, mekanik ve dayanıklılık özelliklerini incelemektedir. Ana hedef, iyi mekanik dayanıklılığa sahip düşük yoğunluklu bir malzeme elde edilmesiydi, ancak bentonit ve PPF'nin birleşimi beklenmedik bir şekilde "köpük çökmesi" sorununa neden olmuştur. Bentonitin yüksek su emilimi ve PPF'lerin oluşturduğu fiziksel ağ, hamurun akma gerilmesini kritik bir seviyenin üzerine çıkarmış ve karıştırma sırasında köpük kabarcıklarının bozulmasına neden olmuştur. Sonuç olarak, karışımlar iki ayrı gruba ayrılmıştır: (1) Düşük yoğunluklu (641 kg/m³), yüksek gözeneklilikli (61,2%) ve mükemmel ısı yalıtımına (0,172 W/mK) sahip, ancak düşük basınç dayanımına (2,32 MPa) sahip kararlı GFC'ler (ör. 0BP5); ve (2) Daha yüksek yoğunluklu (1779 kg/m³), daha yüksek dayanımlı (20,56 MPa) ve daha iyi donma-çözülme direncine (kütle kaybı %1,84) sahip yoğunlaştırılmış harçlar (ör. 20BP5), ancak yalıtım özelliklerini kaybetmişlerdir (0,543 W/mK). Ek olarak, yüksek sıcaklık testleri bentonitin 750 °C'de termal stabiliteyi önemli ölçüde iyileştirdiğini göstermiştir. Sonuç olarak, bulgular reolojinin kontrol edilmesinin GFC geliştirmede yalıtım ve mukavemet dengesini sağlamada anahtar rol oynadığını vurgulamaktadır.

1. INTRODUCTION (GİRİŞ)

Although the construction industry is the backbone of modern civilization, it faces significant environmental sustainability challenges [1]. In particular, the production of ordinary Portland cement (OPC) is considered a primary cause of environmental deterioration, as it requires high energy consumption and emits large amounts of carbon dioxide (CO2) [2]. The increasing demand for energy-saving, sustainable, and lightweight building materials necessitates exploring

*Corresponding author, e-mail: gkaplan@atauni.edu.tr
DOI: 10.29109/gujsc.1855241

alternatives to traditional concrete [3]. As a response to such issues, alkali-activated materials (AAM) or geopolymers (GPs) are developed as innovative alternatives to standard cement. Geopolymer technology is based on the principle of alkali activation of aluminosilicate structures. Products synthesized from such reactions exhibit cementing behaviour, including high compressive strength, thermal resistance, and acid resistance, without the need for standard cement [4]. AAM align with global trends to reduce environmental pollution and promote circular-economy principles by enabling the recycling of industrial waste (slag, fly ash, silica fume, red brick waste, and clay soil) [5]. Although geopolymers were initially designed with high strength and durability as target properties, the energy-efficiency demands of modern buildings have created a need to render these materials also light and thermally insulating [6]. In this context, Geopolymer Foam Concrete (GFC) is of particular interest as a new material that combines the advantages of geopolymer binders (sustainability, strength) with the cellular structure of foam concrete (lightness, insulation) [7].

Foam concrete (FC) is a stable and uniform foam-gel-containing cement mortar, typically aggregate-free, formulated with cement, water, filling material, and an appropriate foaming agent [8]. GFC is attractive as it has low specific gravity, high porosity, high fluidity, moderate thermal insulation, and fire resistance [9,10]. The ordinary concrete (OC) density, for example, is 2000–2800 kg/m³, while foam concrete is 300–1800 kg/m³. Moreover, the thermal conductivity of FC is 0.05–0.3 W/mK, whereas that of OC is approximately 2.5 W/mK, indicating FC's superior insulating properties [6]. However, foam concrete's natural high porosity and low density typically result in low tensile strength and brittleness, which is the biggest drawback for structural applications [11]. To offset these drawbacks, scientists incorporated various synthetic and natural fibers into fiber-reinforced foam concrete (FRFC) mixtures [11]. Fresh state foam concrete stability is primarily a function of the foaming agent properties and the cement mortar [12]. It has also been stated that rheology is an essential factor in foam extinction and foam stability in foam concrete [13–15]. To achieve the desired lightweight and insulating qualities, the pre-formed foam must survive within the concrete matrix. Technically, the stability of a geopolymer foam largely depends on the rheological balance of the fresh paste. According to Dhasindrakrishna et al. (2021) [12], a certain yield stress is required to prevent air bubbles from rising to the surface and separating. However, excessive viscosity caused by fine admixtures can lead to the opposite problem, whereby high shear stresses generated during mixing physically tear the bubble films (bubble burst) [6]. Therefore, identifying a 'safe rheological window' is far more critical for geopolymer foams than for conventional concrete. While recent studies have focused on optimising this balance, the specific rheological impact of minerals with high water demand, such as bentonite, on foam systems remains inadequately investigated.

Ground Granulated Blast Furnace Slag (GBFS), the main binder of this study, is one of the most widely used waste materials in the production of alkali-activated materials [16]. GBFS supports the formation of Calcium Aluminosilicate Hydrate (C-A-S-H) gels during alkaline activation, thanks to its high calcium (CaO) content (e.g., 33.7–41.5%) and its pozzolanic activity [17]. Blending GBFS with other precursor materials, such as fly ash (FA), can increase workability and early strength by accelerating the reaction kinetics [18]. In the activation process, the use of one-part alkaline activators provides ease of application and safer use compared to traditional two-part systems (liquid Sodium Silicate and Sodium Hydroxide solution) [19]. In one-part systems, the solid activator (e.g., powdered sodium metasilicate) is mixed with the precursor materials, and activation is initiated by simply adding water [20]. In such systems, R&D studies on the activation of natural pozzolans (clay-based) have increased in recent years. Bentonite is a natural clay mineral consisting mainly of montmorillonite and is used as a partial replacement material in geopolymer production [21]. Studies in the literature have investigated the effect of bentonite on geopolymer properties [22]. It has frequently been observed that the addition of bentonite negatively impacts workability due to its high specific surface area. Bentonite requires more water or an alkaline solution to thoroughly wet the particle surfaces, thereby reducing the mix's flowability. Several studies have shown that high-temperature heat treatment reduces the surface area of bentonite, thereby increasing workability [23]. However, in these systems, where bentonite is predominantly used as a rheology modifier and pozzolanic additive, it also contributes to strength development by forming a microfiller and a second-phase binder in the mortar matrix [21]. 10% replacement of bentonite in fly ash geopolymers has been shown to decrease workability while maintaining mix cohesion [24].

Fibers such as Polypropylene Fibers (PPF) add structural strength and ductility to foam concretes and geopolymers, help prevent crack development,

and reduce brittleness [25]. Studies on fiber-reinforced foam concrete (FRFC) indicated that the addition of fibers can increase tensile strength by 3 times and flexural strength by 4 times [11]. PPF promotes toughness and crack resistance by sealing microcracks. PPF is added at 0.2% to 1.5% of the mix volume [26]. Incorporating the PPF into the mix, however, significantly impacts workability [27]. Fibers increase internal friction within the matrix due to their large surface area, restricting the fluidity of the mortar [28]. Studies have shown a measurable decrease in yield diameter values with increasing PPF content (e.g., from 0.5% to 1%) [29]. This is attributed to the fibers' hydrophobic nature and their ability to inhibit the free movement of particles within the mortar [30]. The literature has separately examined the role of GBFS in geopolymers [31], the individual effects of bentonite on workability and durability [32], and the benefits of PPF on mechanical properties and toughness [33]. There are also studies on GFC systems in which bentonite acts as a rheology modifier and PPF as a network former [34].

While these materials have been studied separately, there is still a significant gap in understanding their combined behavior in lightweight foam concrete systems. Specifically, the interaction between bentonite and PPF within a delicate “single-component” matrix remains poorly understood. Existing research has yet to pinpoint the “critical rheological threshold” where the combination of these additives compromises foam stability and causes structural failure. This study goes beyond typical characterization by systematically exploring how bentonite and PPF induce "foam collapse" through changes in the flow stress of fresh mortar. Its originality and importance come from pioneering the detailed analysis of this collapse mechanism; by identifying the exact rheological limits at which a highly porous, insulating geopolymer transforms into a denser structural mortar, it provides a crucial "design window” for future use.

2. MATERIALS AND METHODS (MATERYAL VE METOD)

2.1. Raw materials (Malzemeler)

Alkali-activated composites were produced in this study using blast furnace slag (GBFS) as the main binder. Physically, it is a fine, cream-colored powder with a high specific surface area (~5300-5445 cm²/g by the Blaine method) and a specific gravity of roughly 2.86-2.89. In this study, GBFS, the main binder, was partially substituted with bentonite, a naturally occurring clay mineral. The GBFS used in this study was supplied by OYAK Ereğli Demir Çelik Fabrikaları T.A.Ş., Zonguldak, Türkiye. Bentonite is an aluminosilicate composed primarily of montmorillonite and containing reactive silicon dioxide (SiO2) and aluminum oxide (Al2O3) necessary for alkali activation. Bentonite as provided by Samaş Sanayi Madencilik A.Ş., Tokat, Türkiye. Its specific gravity is 2.62, and its Blaine fineness is 3550 cm2/g. Chemical properties of GBFS and bentonite are given in Table 1.

Table 1. Chemical properties of GBFS and bentonite (YFC ve bentonitin kimyasal özellikleri)

Component	CaO	SiO2	Al2O3	Fe2O3	Na2O	K2O	MgO	SO3	LOI
GBFS	33.5	39.7	7.6	3.1	0.3	0.7	10.8	0.7	1.5
Bentonite	4.5	60.3	15.9	3.2	2.7	1.6	2.1	0.3	9.3

Silica sand with a particle size range of 0-2 mm was used as the fine aggregate in the geopolymer foam concrete mixtures studied. Silica sand was supplied from a local sand quarry in Kastamonu. Silica sand, whose primary component is crystalline silicon dioxide (SiO2), generally functions as a chemically inert filler material in alkali-activated binder systems1. The specific gravity of the silica sand used was approximately 2.69, and its 24-hour water absorption capacity was measured as 2.1%3. The particle size distribution of the silica sand is given in Figure 1.

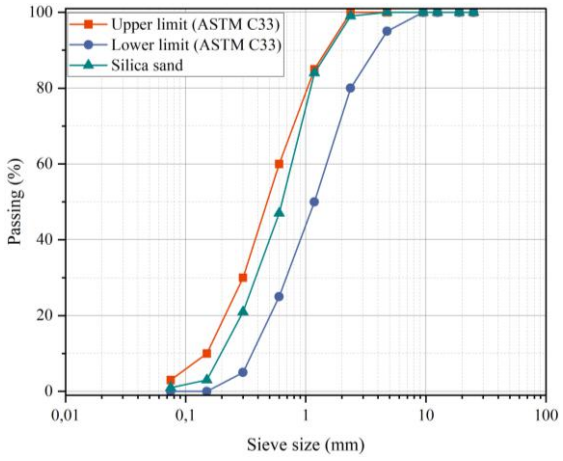

Figure 1. Particle size distribution of silica sand (Silis kumunun dane boyutu dağılımı)

In this study, sodium metasilicate (Na2SiO3) was used in solid (powder) form as a one-part system to provide alkaline activation of aluminosilicate precursors (GBFS and bentonite). One-part activators are premixed solid aluminosilicate and alkali sources that initiate the reaction upon addition of water. In this system, powdered sodium metasilicate dissolves when water is added to the mixture, providing both the alkalinity required for the reaction (as a Na_2O source) and soluble silicate (SiO_2) species. The molecular weight of the powdered sodium metasilicate used is 122.06 g/mol, and its specific gravity is 2.61.

In this study, a sodium lauryl sulfate (SLS)-based foaming agent was used to produce a cellular, lightweight geopolymer foam concrete (GFC) structure. SLS is a widely used anionic surfactant. The agent used in this study had a pH of 5. To produce the foam, SLS was mixed with water at a specific weight ratio (e.g., 95:5 water: SLS) and then foamed using a high-speed mixer. This procedure produced a stable foam that could be mixed into the geopolymer mortar and had a density of about 120 g/L. Powdered sodium metasilicate (Na2SiO3) and SLS used as alkali activators were supplied by Sigma-Aldrich (Germany).

Polypropylene fibers (PPF) were added to geopolymer foam concrete mixtures to improve their mechanical performance, specifically their ductility and crack resistance. Although PPF is a product of Chinese origin, it was supplied by a local supplier. The PPF used in this study were 6 mm long and 17 μm in diameter. Their low density (0.91 g/cm3), as indicated by their physical characteristics, allows them to be used without appreciably raising the composite's overall weight. PPF has a high elongation at break (30%) but a comparatively low modulus of elasticity (3.5 GPa) and tensile strength (300 MPa). These properties enable PPF to bridge microcracks, prevent their formation and propagation within the matrix, distribute stresses more evenly, and enhance the material's toughness and energy absorption capacity. Figure 2 presents the general appearance of the materials used in this study.

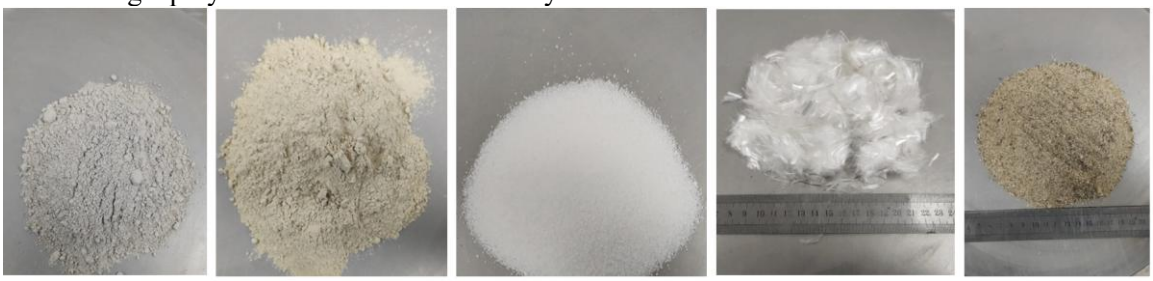

Figure 2. Materials used in GFC production (Köpük beton üretiminde kullanılan malzemeler)

2.2. Mix Design (Karışım Tasarımı)

In this study, bentonite and PPF-added GFC mixtures were designed using a one-part alkali activator. Blast furnace slag (BFS) was used as the primary aluminosilicate source, and three main groups of mixtures were created, with GBFS being replaced by bentonite at 0%, 10%, and 20% by weight. The total binder content (BFS + Bentonite) was kept constant at 700 kg/m3 in all mixtures. According to the one-part system principle, sodium metasilicate was used as a powder to ensure alkali activation. In all mixtures, the sodium metasilicate content was maintained at 15% of the total binder weight (105 kg/m3). A constant mixing water content of 210 kg/m³ was used for each batch of fresh geopolymer paste, corresponding to a water-to-binder ratio of 0.30. It should be explicitly stated that this value refers strictly to the water used to activate and achieve the desired workability of the paste.

The 210 kg/m³ of mixing water does not include the water in the pre-formed foam, which was prepared separately and added at a volume of 60 kg/m³. This is because the foam is introduced as a separate volume component, similar to a lightweight aggregate. Preliminary experiments were conducted to determine the water content and water-to-binder ratio of the mixtures. To create the foam structure, 60 kg/m³ of foam made with an SLS-based foaming agent was added to each mixture. Depending on the polypropylene fiber ratio, silica sand in the 0-2 mm size range was used as fine aggregate in quantities ranging from 238.7 kg/m³ to 276.2 kg/m³. PPF was added to the blends at three different volumetric rates to enhance their mechanical properties: 0% (control series without fibers), 0.5% (PPF = 0.5%; 4.6 kg/m³), and 1% (PPF = 1%; 9.1 kg/m³). Based on the fiber density, these rates represent the target volumetric fractions (Vf) of the foam concrete mixture relative to its total volume.

Table 2. Material ratios (%) and weights (kg/m^3) used in GFC production (Köpük beton üretiminde kullanılan malzeme yüzdeleri (%) ve ağırlıkları (kg/m^3)

Mix ID	Bentonite (%)	PPF (%)	GBFS	Bentonite	Water	Sodium metasilicate	Foam	Silica sand	PPF
0BP0	0	0	700	0	210	105	60	276,2	0,0
10BP0	10		630	70	210	105	60	271,0	0,0
20BP0	20		560	140	210	105	60	265,9	0,0
0BP5	0	0.5	700	0	210	105	60	262,6	4,6
10BP5	10		630	70	210	105	60	257,4	4,6
20BP5	20		560	140	210	105	60	252,3	4,6
0BP10	0	1	700	0	210	105	60	249,0	9,1
10BP10	10		630	70	210	105	60	243,8	9,1
20BP10	20		560	140	210	105	60	238,7	9,1

2.3. Preparation, mixing and curing of samples (Numunelerin hazırlanması karıştırılması ve kürlenmesi)

A standard laboratory mixer was used to prepare geopolymer foam concrete mixtures. First, the specified proportions of solid binders (GBFS and Bentonite) and a one-part alkali activator (Sodium Metasilicate) in powder form were placed in the mixer vessel and mixed homogeneously at low speed (approximately 145 rpm) for 1 minute. The calculated amount of mixing water was then added, and the mixture was mixed first at low speed (145 rpm) for 1 minute, then at high speed (approximately 280 rpm) for another 3 minutes, resulting in a fluid geopolymer paste. Simultaneously, the SLS foaming agent and water were mixed in a high-speed mixer at the specified ratio to produce a stable foam with a density of approximately 120 g/L. The foam was added to the prepared geopolymer paste and gently mixed first at low speed (145 rpm) for 1 minute to prevent disruption of the foam structure, and then at high speed (280 rpm) for 2 minutes. Polypropylene fibers (PPF) were then added to the specified amounts for each mixture, and the mixtures were mixed for 1 minute at low speed (145 rpm) and 3 minutes at high speed (280 rpm) to ensure homogeneous fiber distribution. Finally, silica sand was added to the mixture, and mixing was completed for 1 minute at low speed (145 rpm) and 2 minutes at high speed (280 rpm) to ensure final homogeneity.

Fresh geopolymer foam concrete mixtures were poured into steel molds of the standard dimensions required for the tests (e.g., a 50x50x50 mm cube for compressive strength and a 40x40x160 mm prism for flexural strength). The molds were filled homogeneously. Immediately after pouring, the surface was smoothed, and the moulds were covered with stretch film to prevent moisture loss.

After casting, the moulds were placed in an oven to cure immediately. The samples were heated to 75°C at a controlled rate of 5°C per minute and maintained at this temperature for 24 hours. Once the curing period ended, the oven was turned off to avoid thermal shock, allowing the samples to cool gradually to room temperature inside the closed oven over about 12 hours. The specimens were then carefully removed from the mould exactly 36 hours after casting and stored in standard laboratory conditions (20°C and 50% humidity) until testing.

2.4. Test Methods (Test Yöntemleri)

Fresh GFC mix flowability was tested using a spreading table in accordance with ASTM C1437. The fresh mortar was immediately poured into a standard conical mould placed directly in the center of the spreading table after mixing. After smoothing the surface, the mould was carefully removed, and the table was dropped 25 times to measure the spreading diameter (in two perpendicular directions). The average of these two values was considered the spreading diameter of the mix (in mm). The fresh density of the mixes was determined using a container of known volume. The fresh GFC was immediately poured into a known-volume container (a standard mould with dimensions 50x50x50 mm) without compacting (or at a level low enough to avoid disrupting the foam structure). The top surface was leveled with a straight edge, then the container was scraped off, and afterwards the GFC and the GFC inside were weighed. The net weight of the GFC was obtained by subtracting the container weight. The weight was used to divide the container's volume to calculate the fresh density (kg/m^3).

Physical characteristics, such as apparent porosity, water absorption capacity, and oven-dry unit volume weight, of cured geopolymer foam concrete

(GFC) specimens were tested in accordance with ASTM C642 using 50 x 50 x 50 mm cube specimens that had completed the standard curing period (28 days). During the test procedure, the samples were first dried at 50°C in an oven for at least 72 hours to a constant weight. A precision balance was used to measure the samples' oven-dry weight after they were oven-dried and cooled to room temperature. The dry weight was then divided by the sample volume to find the oven-dry unit weight (hardened density).

Subsequently, the samples were fully immersed in room-temperature water (approximately 21°C) to saturate and were held for at least 48 hours. The samples were then removed from the water, wiped with a moist cloth, and their saturated-surface-dry (SSD) weights (WSSD) recorded. Water absorption capacity, expressed as a percentage of the sample weight, was calculated using the following formula: $WA = (WSSD - WD) / WD \times 100$.

Measurable porosity, which is the ratio of open pores to the sample volume, was determined following procedures in the ASTM C642 standard. This value reflects the material's internal pore structure.

Flexural and compressive strength were tested at the end of the established curing times (7 and 28 days) to quantify the samples' mechanical performance. Flexural strength was calculated from 40 x 40 x 160 mm prismatic test specimens. The tests were conducted using the three-point bending method in accordance with ASTM C348. Test specimens were set up in a variable support span test machine, and the center of each specimen was subjected to a constant load of 50 N. Using standard equations, the flexural strength in MPa was determined after the maximum failure load was recorded. The average of at least three specimens for each mixture and curing age was used to report the results. Compressive strength tests were conducted on the broken prism fragments (approximately 40x40 mm cross-section) obtained from the flexural strength test, in accordance with ASTM C349 standard. Two pieces obtained from each prism were placed between loading plates, and the load was applied at a constant rate (0.6 MPa/s) until the specimen broke. The maximum load at the moment of fracture was recorded, and the compressive strength (in MPa) was calculated by dividing the load by the loading area of the specimen. The compressive strength was determined by averaging the six flexural test pieces for each mixture and curing age. Mechanical performance tests (compression and bending) were carried out using a UTest LC 815 Universal Testing Machine (Ankara, Türkiye).

Sorptivity tests were carried out in accordance with TS EN 1015-18 to determine the water absorption rate of hardened GFC samples through capillary voids. Cube samples measuring 50x50x50 mm that had completed a 28-day curing period were used for this test. Before the test, the samples were dried in an oven at 50 ºC for 3 days to remove moisture. Subsequently, the sample sides were treated with a water-repellent coating (paraffin) to prevent water absorption. The samples so treated were then immersed in a tray so that their bottom faces contacted about 5 mm of water. The capillary water-absorption properties of the samples were determined after 24 hours of storage under these conditions. The thermal conductivity coefficients were determined to establish the samples' thermal insulation behaviour. 500 x 500 x 30 mm-sized plate samples were conditioned for the test. The samples were oven-dried at 50°C for 3 days, starting on the 28th day of curing, to remove water. Steady-state thermal conductivity experiments were performed using a heat flow meter in accordance with ASTM C518. Under the test, a controlled temperature gradient was applied to the two surfaces of the sample, and the heat flux through the sample was measured. Steady-state thermal conductivity measurements were performed using a LINSEIS SFM 300 thermal conductivity analyser (Selb, Germany).

The samples subjected to the standard curing time (28 days) were exposed to various temperatures to analyse the performance and heat stability of geopolymer foam concrete (GFC) mixtures at high temperatures. For this test, 50x50x50 mm cube samples were used. To simulate fire conditions and the effects of high temperatures, the samples were heated in a PROTHERM PLF 160/9 programmable laboratory muffle furnace (Ankara, Turkey). The temperature of the furnace was raised to the target temperature zones (250°C, 500°C, and 750°C) with a heating rate of 10 ºC/min. After reaching the target temperature, the samples were held at that temperature for 2 hours. After the hold period, the furnace was shut down, and the samples were air-cooled to room temperature in the furnace. After cooling, the samples' weights were measured, and the percentage mass loss due to the high-temperature effect was calculated. Residual compressive strength (compressive strength) of the samples was determined based on ASTM C349. These were conducted to determine the structural

capacity and mechanical performance of the materials under different temperature conditions.

Tests were conducted to assess the resistance of geopolymer foam concrete (GFC) mixtures to cyclic freezing and thawing, in accordance with the freezing-thawing temperature regime specified in ASTM C666. However, the duration was limited to 30 cycles to accommodate the foam samples' highly porous nature. However, preliminary trials and literature showed that the 300-cycle duration specified in the standard would completely compromise the structural integrity of the tested 'stable geopolymer foam concrete' samples, due to their high porosity (over 50%) and low density. This made it impossible to complete the measurement. To prevent the material from becoming overly aggressive and disintegrating entirely, and to allow meaningful comparisons between the stable foams and dense mortars, the test was limited to 30 cycles. The test specimens had undergone the customary 28-day curing period and measured 50 x 50 x 50 mm. Before the test, the samples were saturated with water. Afterward, they were subjected to a programmable freeze-thaw cycle in a chamber. In a cycle, the samples' core temperature was lowered from +4°C to -18°C (the freezing phase) and then progressively raised back to +4°C (the thawing phase) over a predetermined time, typically 2 to 5 hours. The samples were then removed from the chamber and visually examined for cracking, scaling, or chipping. Their weight was measured, and the percentage mass loss due to the cycles was determined. The samples' compressive strength was then determined. These tests were primarily designed to provide an initial evaluation of the composites' resistance to frost deterioration under cyclic freezing and thawing conditions. Freeze-thaw resistance tests were carried out using a fully automated U-Test UTD-1440 freeze-thaw chamber (Ankara, Türkiye).

A total of nine different mixes were designed based on these variables. Mix IDs were coded to reflect the percentages of bentonite and polypropylene fiber they contained (for example, code 10BP5 represents a mix containing 10% bentonite and 0.5% PPF). Detailed material quantities for all mixes are presented in Table 2.

3. RESULTS AND DISCUSSIONS (BULGULAR VE TARTIŞMA)

3.1. Fresh Properties (Taze Hal Özellikleri)

The measured flow diameters, which indicate the workability of the fresh GFC mix, decreased with increasing polypropylene fiber (PPF) concentration and the bentonite replacement factor (Figure 3). The effect of the PPF added was the most negative. For example, in the bentonite-free (0%) series, the 0BP0 mix had a highly spread diameter of 215 mm. However, the value reduced to 126 mm (a reduction by 41.4%) in the presence of 0.5% PPF (0BP5) and to 83 mm (a decrease by 61.4%) in the presence of 1% PPF (0BP10). This decrease is due to the fibers forming a three-dimensional network in the fresh mortar, increasing internal friction and hindering the mortar's flow. The high surface area of the fibers directly influences the mix rheology, with increased yield stress and decreased workability [35,36].

The flow diameter decreased as the bentonite replacement ratio (0–20%) increased for all fiber contents (0, 0.5, and 1 PPF). For example, 0% bentonite (0BP0) measured 215 mm in the series without PPF (0% PPF), while 20% bentonite (20BP0) reduced it to 176 mm, representing an 18.1% decrease. Montmorillonite, the primary mineral in bentonite, has a layered crystal structure and a high specific surface area. Bentonite swells through water absorption, reducing the paste's effective water/binder ratio. This significantly increases the yield stress and viscosity of the fresh geopolymer paste, restricting its flowability [21,23]. The lowest flow values, as anticipated, were observed for the 20BP10 mix (68 mm), which had the highest bentonite content (20%) and fiber content (1%). That is to say, the subsequent increase in viscosity caused by bentonite's water-absorbing property, coupled with the internal friction generated by the PPF (synergistic effect), effectively reduced the mix's flowability.

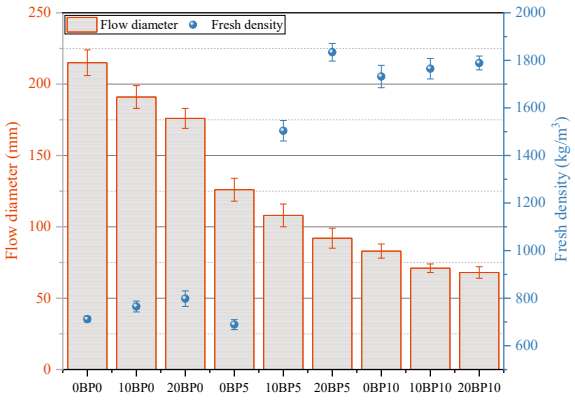

Figure 3. Fresh state properties of fresh GFC mixtures (Köpük beton karışımlarının taze hal özellikleri)

The fresh density tests recorded the most striking results of the study. The addition of fiber and bentonite was found to affect the stability (collapse of foam) of preformed foam directly by modifying the rheology of the geopolymer paste. In the reference batch without fibers (0% PPF), the fresh density increased by only 12.1% (from 712 kg/m3 to 798 kg/m3), while the bentonite proportion was raised from 0% to 20%. This indicates that the increased viscosity of the bentonite caused mechanical destruction of the foam bubbles during mixing, but had no effect on the global foam structure. This equilibrium changed completely once PPF was incorporated. With 1% addition of PPF (0BP0 to 0BP10), the fresh density increased from 712 kg/m3 to 1732 kg/m3 (143.3% increase). It indicates that the network formed by the fibers significantly increases the shear resistance of the fresh paste, and that this high resistance mechanically bursts foam bubbles within the fresh foam during mixing (bubble bursting) [37,38]. In this study, fibers were added to the mixture after foam formation to ensure uniform fiber distribution. However, the sudden collapse of foam seen in mixtures with high levels of bentonite and fibers (e.g., 20BP5 and all PPL=1 series) is believed to be caused not only by rheological changes (high yield stress) but also by the mixing sequence. Adding fibers after foaming led to direct physical contact and friction between the fibers and the delicate foam bubbles during mixing. The increased viscosity of the bentonite matrix sped up this mechanical effect, causing the bubbles to burst. Therefore, the 'conversion to dense mortar' mechanism reported here results from both the material composition (bentonite and fiber) and the process used (mixing sequence).

The most striking effect was seen in the PPF = 0.5 series. In this series, the density at 0% bentonite content (0BP5) was as low as 689 kg/m3, but the addition of 10% bentonite (10BP5) increased the density to 1504 kg/m3 (118.3% increase) and to 1834 kg/m3 (166.2% increase) with the addition of 20% bentonite (20BP5). These results strongly support the "foam extinction" hypothesis. The mechanism is the exceedance of a critical threshold between the paste's rheology and the foam's mechanical stability. Bentonite, through its high water absorption capacity, increases the paste's yield stress [24]. On the other hand, PPF further increases the paste's shear resistance and viscosity by forming an internal network structure [39]. When these two effects combine (especially in mixes 10BP5, 20BP5, 0BP10 and above), the rheology of the fresh mortar becomes so "hard" and "resistant" that the stable foam bubbles formed with SLS cannot withstand the mixing forces under high shear stress and mechanically collapse (burst).

Fu et al. (2020) stated that very low water content (or water binding to materials such as bentonite) results in a "stiff mixture that readily leads to bubble bursting." [40]. Dhasindrakrishna et al. (2021) argued that foam collapse is rheologically dependent but is caused by a very low yield stress (drainage) [12]. This study, however, clearly demonstrates the opposite mechanism: mechanical bursting due to an excessively high yield stress.

As a result, mixtures containing 0.5% PPF and over 10% bentonite (or all mixtures containing 1% PPF) deviated from the intended "foam concrete" structure due to the almost complete slaking of the foam. They transformed into a "fiber-reinforced densified geopolymer mortar" structure. This is particularly evident at fresh densities as high as 1834 kg/m3.

3.2. Physical Properties (Fiziksel Özellikler)

The apparent porosity and oven-dry hardened density (unit weight) values measured after 28 days

of curing show a strong, direct correlation with the fresh-state observations (Section 3.1). It was found that increases in fresh density resulted in increases in hardened density and a dramatic decrease in apparent porosity (Figure 4). This demonstrates that foam collapse in the fresh mix is the primary factor determining the final pore structure of the hardened material.

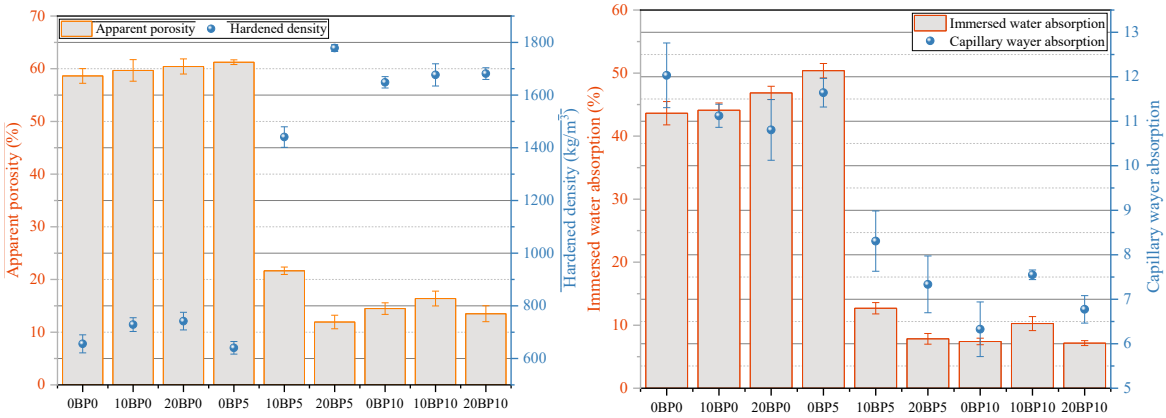

(a) Apparent porosity- Hardened density

(b) Water absorption behaviors

Figure 4. Physical properties of fresh GFC mixtures (Köpük beton numunelerinin yaş hal fiziksel özellikleri)

Fiber-free 0BP0, 10BP0, and 20BP0 mixtures exhibited high, similar porosity values of 58.6%, 59.7%, and 60.4%, respectively (Figure 4a). This high porosity ensures that the series maintains a favorable foam concrete structure. The slight increase in porosity with bentonite addition can be explained by bentonite's high water requirement, which has the potential to create more capillary pores (nanoscale capillary pores) in the solid matrix [41,42]. The porosity of the 0BP10 mixture with 1% PPF is just 14.5%. That is a reduction of 75.3% from the 58.6% porosity of 0BP0. That is an enormous drop, which indicates that the foam structure has completely disappeared, transforming the material into solid, rather than porous, mortar. The foam collapse is most clearly seen in the PPF = 0.5% series. The 0BP5 mix with 0.5% PPF was the most porous in the series at 61.2% (stable foam). Porosity dropped to 21.7% with the addition of 10% bentonite (10BP5) and 11.9% with the addition of 20% bentonite (20BP5). That is an 80.6% drop in porosity relative to the 0BP5 control mix.

The hardened density results clearly demonstrate the degrading effect of the fiber-bentonite synergy on the foam structure (Figure 4b). In the series free of fibers (0BP0, 10BP0, 20BP0), a reasonable hardened density of 13.1% was recorded, ranging from 656 kg/m3 to 742 kg/m3, as bentonite replacement ranged from 0% to 20%. These align with typical lightweight foam concrete densities of 600-800 kg/m3. This means that bentonite alone (in the absence of fibers) will not cause catastrophic failure of the foam structure but will marginally increase the paste density [40,43]. The 0BP10 mixture containing 1% PPF but no bentonite consisted of a density of 1648 kg/m3. When compared with the density of the control (0BP0) mixture in the absence of fibers (656 kg/m3), it was observed that inclusion of fibers alone had increased the density by 151.2%. This finding confirms that the 1% PPF alone can mechanically destabilize foam bubbles during mixing, increasing the internal friction and shear resistance of the fresh paste [44,45]. As the foam structure had already been destroyed in this batch (0BP10, 10BP10, 20BP10), the addition of bentonite increased the density only slightly (from 1648 to 1681 kg/m3). Most significantly, the result in the series was 0.5% PPF. In the 0BP5 mixture, prepared with 0.5% PPF but without bentonite, a stable foam concrete was achieved with a density of 641 kg/m3. However, when 10% bentonite was added to this mix (10BP5), the density increased to 1441 kg/m3 (a 124.8% increase), and when 20% bentonite was added (20BP5), the density increased to 1779 kg/m3 (a 177.5% increase).

These results unequivocally confirm the mechanical collapse hypothesis proposed in the analysis of fresh properties. While 0.5% PPF (0BP5) or 20% bentonite (20BP0) alone did not disrupt the rheology sufficiently to cause foam collapse, their combination produced a synergistic effect. The high water absorption capacity of bentonite significantly increased the paste's viscosity and yield stress, while 0.5% PPF added internal friction to the already hardened mortar. Consequently, the shear

resistance of the fresh mortar in these mixtures (10BP5 and 20BP5) increased to the point that foam bubbles could no longer remain stable during mixing, and the structure collapsed [24].

The results of immersed water absorption and capillary water absorption tests are given in Figure 4b. All blends in the fiber-free (0% PPF) series (0BP0, 10BP0, 20BP0) and the 0BP5 blend containing 0.5% PPF exhibited exceptionally high water absorption values, ranging from 43.6% to 50.4%. This is clear evidence that these blends maintain a foam structure with low density (~641-798 kg/m3 in the previous analysis) and a high degree of open (interconnected) porosity. Water readily infiltrates this network of interlinked macropores, filling the matrix [46]. The fact that the 0BP5 blend with the highest porosity (61.2%) also had the highest water absorption (50.4%) in this set further supports the direct correlation. The mixtures that exhibited foam collapse (10BP5, 20BP5, 0BP10, 10BP10, and 20BP10) showed the most substantial evidence. The water absorption levels of these mixtures ranged from 7.2% to 12.7%, which are remarkably low. For example, adding 20% bentonite (20BP5) reduced the water absorption rate to 7.8%, down from 50.4% in the 0BP5 mix (0.5% PPF). This represents an astounding 84.5% decrease in water absorption capacity.

Capillary water absorption (sorptivity) testing measures how quickly a material absorbs water by capillary suction and is a key indicator of durability [47]. The foams with stable foam structure (0BP0, 10BP0, 20BP0, and 0BP5) possessed extremely high sorptivity values ranging from 10.8 kg/m2 to 12.0 kg/m2. The high, open-pore structure provided ample pathways for rapid water absorption via capillary action [39]. Notably, in the 0% PPF series, the overall water absorption was greater with an increase in the content of bentonite from 0% to 20%, whereas sorptivity (the rate of capillary water absorption) decreased from 12.0 to 10.8 kg/m². This shows the bivalent character of bentonite: On the one hand, its swelling when it absorbs water and its significant water demand lead to increased total water absorption. On the other hand, it functions as a filler, stimulating geopolymer gel (N-A-S-H) development and thereby enhancing the matrix's capillary pores (pore refinement) [48,49]. This thinning lowered the water intake rate. As expected, the dense mixtures in which the foam had collapsed exhibited extremely low sorptivity values (6.3-8.3 kg/m2). The lowest value, 6.3 kg/m2, was recorded for the 0BP10 mixture (which contained only 1% fiber). The 37.1% reduction from 0BP5 (stable foam, 11.6 kg/m2) to 20BP5 (collapsed foam, 7.3 kg/m2) strongly indicates a microstructural transformation.

Water absorption and sorptivity tests were in excellent agreement with the findings of fresh and hardened density. The combined use of bentonite and polypropylene fibers above a certain threshold (0.5% PPF and 10% bentonite, or 1% PPF) increased the rheology (viscosity and yield stress) of the fresh mortar to levels beyond the foam bubbles' tolerance. This resulted in mechanical foam collapse during mixing, increasing the density from 650 kg/m3 to 1800 kg/m3 and decreasing the porosity from 60% to 12%.

3.3. Mechanical Properties (Mekanik Özellikler)

The 7- and 28-day compressive strength results for the mixtures reveal the complex, synergistic effects of bentonite and PPF on the mechanical performance of the composite (Figure 5a). The mixtures 0BP0, 10BP0, 20BP0, and 0BP5, which were found to maintain a stable foam structure (low density, high porosity), showed low compressive strength values , as expected. The 28-day strengths ranged from 2.32 MPa to 3.83 MPa. These values are consistent with the typical strength range for geopolymer foams reported by Ahıskalı et al. (2025) of 2-12 MPa [39]. As the bentonite replacement rate increased (from 0% to 20%), a 18.1% decrease in 7-day strength was observed, from 2.32 MPa to 1.90 MPa. This can be explained by bentonite's high water absorption capacity, which slows early-age reactions by binding the free water required for geopolymerization and slag hydration. At 28 days, the pozzolanic activity of bentonite became apparent. The 10BP0 mixture containing 10% bentonite reached a 28-day strength of 3.83 MPa, 30.3% higher than the control (0BP0, 2.94 MPa) mixture. This increase is associated with bentonite dissolution in alkaline media, the formation of additional binding gels (N-A-S-H or (N, C)-A-S-H), and the strengthening of pore walls [21]. However, the fact that this increase did not remain at the 10% level (less than 10BP0) with 20% bentonite (20BP0) (3.37 MPa) indicates the existence of an optimal substitution rate.

The changes in the series using 0.5% PPF differ. While the stable foam, 0BP5 (without bentonite), showed a strength of only 2.32 MPa at 28 days, the addition of 20% bentonite (20BP5) increased the strength to 20.56 MPa. This is a massive 786.2% increase. This result mechanically proves that the material is no longer foam concrete but a dense mortar with an 80.6% loss in porosity (Section 3.2) and a density of 1779 kg/m3 (Section 3.2). The

addition of 1% PPF alone also confirmed that it ruptured the foam in the 0BP10 mix. Compared to the 0BP0 mix without fibers (2.94 MPa), the 0BP10 mix containing 1% PPF achieved a 28-day strength of 13.57 MPa (a 361.6% increase). This demonstrates that 1% PPF is sufficient to mechanically rupture the foam, increasing the shear resistance of the fresh mortar.

Within the dense mortar structure, polypropylene fibers acted via a crack-bridging mechanism, preventing the propagation of microcracks that formed under load. This increased both the material's strength and ductility. The literature reports that PPF improves mechanical properties in this way [50,51]. In the 1% PPF series, where the foam had already collapsed, the effect of bentonite addition was clearly visible. 0% bentonite (0BP10) showed a strength of 13.57 MPa, while 10% bentonite (10BP10) increased it to 15.26 MPa, and 20% bentonite (20BP10) to 18.53 MPa. In other words, adding 20% bentonite to these dense mortars containing 1% PPF increased the strength by an additional 36.6%. This indicates that bentonite is no longer a rheology disruptor, but rather a pozzolan that reacts in alkaline environments and acts as a "filler" (physical filler) that fills microvoids in the matrix [44].

Physical filling cannot be the sole reason for the observed increase in strength in this study. The mechanical strength of the matrix was enhanced by the presence of calcium-rich C-A-S-H gels, formed from slag (GBFS) hydration, and N-A-S-H gels, produced by the reaction between bentonite and the activator. By serving as nucleation sites for the geopolymerization products, bentonite particles promoted gel formation and created a denser matrix.

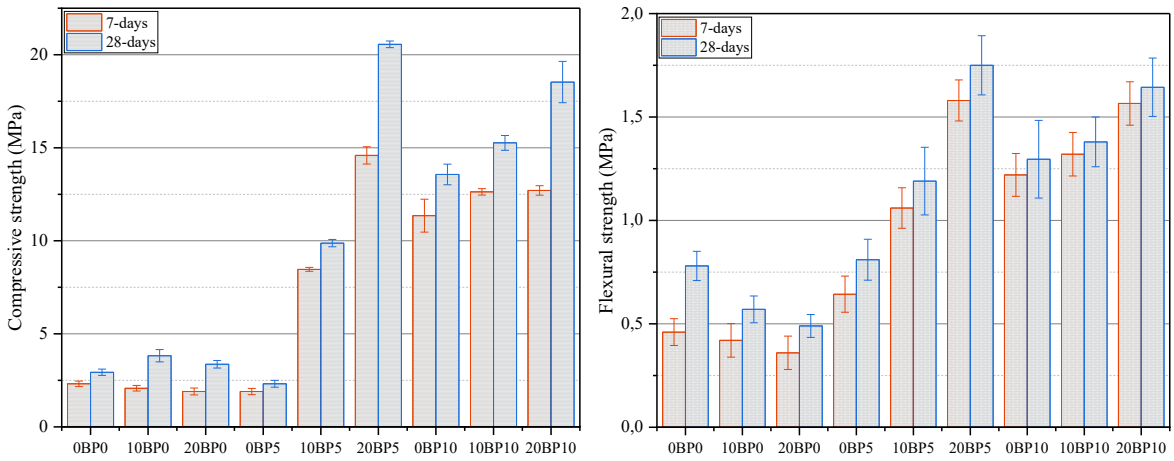

(a) Compressive strength

(b) Flexural strength

Figure 5. Mechanical properties of fresh GFC mixtures (Köpük beton karışımlarının mekanik özellikleri)

The flexural strength results confirm, with striking clarity, the fundamental finding from the compressive strength and physical property analyses: the foam collapse phenomenon (Figure 5b). Mixtures that maintained a stable foam structure (low density) exhibited low flexural strength values as expected (range 0.49 - 0.81 MPa at 28 days).

In the fiber-free (0% PPF) series, increasing the bentonite replacement (from 0% to 20%) decreased the 28-day flexural strength from 0.78 MPa (0BP0) to 0.49 MPa (20BP0). This is a significant 37.2% decrease. This suggests that the pozzolanic contribution observed in compressive strength with 10% bentonite is not relevant to flexural strength. The high water-absorption capacity of bentonite is thought to make the foam pore walls more brittle, reducing their resistance to tensile stress. The 0BP5 mixture containing 0.5% PPF (0.81 MPa) showed a slight increase of 3.8% at 28 days compared to the control mixture without fibers (0BP0 - 0.78 MPa). This indicates that 0.5% PPF remains within the stable foam matrix without deteriorating the rheology (without quenching the foam), bridging microcracks in the pore walls (crack-bridging), and making a positive, albeit minimal, contribution to the material's ductility [24,52].

The 0BP10 mix (1.30 MPa) containing 1% PPF had a 66.7% higher flexural strength than the 0BP0 mix (0.78 MPa) without fibers. This is further evidence that the 1% PPF dosage mechanically collapses the foam, thus densifying the material. Comparing the

stable foam 0BP5 (0.5% PPF) mix (0.81 MPa) with the 20BP5 mix (1.75 MPa) containing 20% bentonite in this series, a 116% increase in 28-day flexural strength was observed. This increase was directly related to a 177.5% increase in density and an 80.6% decrease in porosity. Within this dense matrix, PPF, as in standard fiber-reinforced concrete, resisted the tensile stresses generated under flexural loading and prevented microcracks from coalescing into macrocracks. This crack-bridging mechanism increased the material's flexural strength [53].

The notable rise in flexural and compressive strength highlights the mechanical role of PPF in the dense geopolymer matrix, especially their crack-bridging effect. However, due to limitations in the testing equipment, which affected precise displacement measurements, it was not possible to produce definitive stress-strain curves or toughness and ductility indices in this study. Despite this limitation, future micromechanical studies are suggested to examine the post-peak behaviour and energy absorption of these "extinguished" dense geopolymer composites, aiming to evaluate the ductility enhancement from the fibre-bentonite interaction fully.

In this study, the proposed reaction mechanisms are based on the principle of "chemical equivalence", as summarised in the reference literature [24,44]. Examining the oxide compositions listed in Table 1, it is evident that the GBFS and bentonite used have Ca/Si and Si/Al ratios similar to those reported in the aforementioned studies [54–56]. Since these oxide ratios are primary factors influencing reaction kinetics and product (gel type) formation in alkali-activated systems, the referenced microstructural data are considered representative and applicable to this study.

3.4. Thermal Performance (Isıl Performans)

The fiber-free (0% PPF) series and the 0BP5 blend containing 0.5% PPF exhibited very low thermal conductivity values ranging from 0.172 to 0.188 W/m.K (Figure 6). These values confirm that these blends maintain their high porosity (58.6% to 61.2%) and low density (641 to 742 kg/m3). The material's insulating performance is primarily provided by these stable air voids [57]. Song et al. (2025) reported a value of 0.0914 W/m.K for a foam concrete with a density of 600 kg/m3. The value of 0.172 W/m.K obtained in the 0BP5 (641 kg/m3) mix in this study is close to these ultra-low values, indicating that the material is a good insulator [58].

In the fiber-free series (0BP0, 10BP0, 20BP0), a slight 5.6% increase in thermal conductivity from 0.178 to 0.188 W/m.K was observed as the bentonite content increased. This was paralleled by a 13.1% increase in hardened density. Bentonite slightly increased heat transfer by densifying the pore-wall matrix. The 0BP5 blend (0.172 W/m.K) gave the lowest thermal conductivity value in the series. This suggests that 0.5% PPF contributes to insulation performance by remaining in the matrix without disrupting the foam structure and, perhaps, by stabilizing the pore distribution.

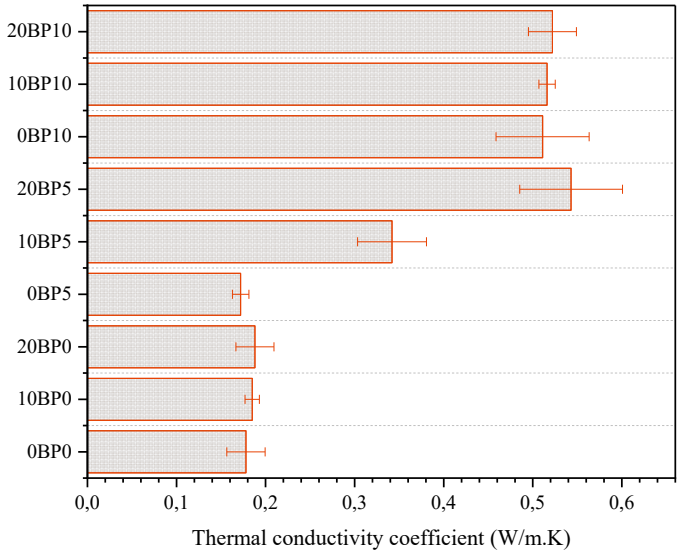

Figure 6. Thermal conductivity coefficients of GFCs (Köpük betonların ısıl iletkenlik değerleri)

The thermal conductivity of the 0BP10 (0.511 W/m·K) mixture containing 1% PPF is 187% higher than that of the 0BP0 (0.178 W/m·K) mixture without fibers. This demonstrates that 1% PPF

alone disrupts the rheology of the fresh mortar, causing the foam structure to collapse and reducing the material's insulating properties. The fact that the values in this series (0BP10, 10BP10, 20BP10) are so close to each other (0.511-0.522 W/m·K) is also noteworthy, as the foam had already collapsed, and the addition of bentonite only slightly increased the conductivity of the dense matrix. Thermal conductivity test results, in conjunction with all previous physical and mechanical data, clarify the main finding of this study: the combined use of bentonite and polypropylene fibers significantly affects the rheology (viscosity and yield stress) of the fresh GFC paste. Exceeding a threshold (0.5% PPF + 10% bentonite, or 1% PPF) raises the shear resistance of the fresh mortar beyond the foam bubbles' capacity, leading to mechanical foam collapse during mixing. As a result, these materials, initially intended for insulation, were transformed into dense geopolymer mortars with high density, high strength, and high thermal conductivity.

3.5. High-temperature resistance (Yüksek Sıcaklık Dayanıklılığı)

The compressive strength values obtained as a result of the high temperature effect of GFC samples are given in Figure 7a. A significant increase in compressive strength was observed in all samples after exposure to 250°C, which had completed 28 days of curing. In the stable foam series, the 0BP5 (0% bentonite, 0.5% PPF) mixture showed the highest proportional increase of 52.2%, from 2.3 MPa to 3.5 MPa. In the dense mortar series, where the foam was deflated, the 10BP5 (10% bentonite, 0.5% PPF) mixture increased from 9.9 MPa to 13.2 MPa (33.3% increase), and the 0BP10 (0% bentonite, 1% PPF) mixture increased from 13.6 MPa to 16.5 MPa (21.3% increase).

This strength increase is a known behavior of alkali-activated systems (AAM). The initial 24-hour thermal cure at 75°C, followed by 28 days at room temperature, was not sufficient to fully react all the reactive aluminosilicates in the system (especially GBFS and bentonite). The 250°C temperature served as an additional thermal post-curing agent for these unreacted particles. This extra thermal energy reactivated geopolymerization, promoting the formation of more binder gels (C-A-S-H and N-A-S-H), further densifying the microstructure and strengthening pore walls, thus increasing strength [59,60].

Following this peak at 250°C, strength loss began in all mixtures as expected as temperatures increased to 500°C and 750°C. This degradation can be explained by two primary mechanisms: First, high temperatures (300-600°C) cause the chemically bound water in the geopolymer gel structure to evaporate. This dehydration leads to shrinkage and internal stresses in the matrix, resulting in microcracks and reduced strength [59]. This is the most critical degradation mechanism for the fibrous blends studied. Second, PPF, as noted by Ahıskalı et al. (2025), has a low melting point (~160-170°C). At 250°C, the fibers are already molten [39]. At 500°C and 750°C, these fibers completely combust and decompose. This leaves voids and microchannels (6 mm long) within the matrix where fibers previously occupied.

In the groups without foam collapse, PPF was either absent (0BP0, 10BP0, 20BP0) or very low (0BP5). Therefore, the primary degradation mechanism at 750°C was matrix dehydration. Consequently, the relative strength loss at 750°C (relative to the 28-day control values) of these blends was more moderate. For example, the 0BP5 blend was 2.3 MPa at 28 days, compared to 2.0 MPa at 750°C (a 13.0% loss). The high 28-day strengths of the foam-slaked blends (e.g., 0BP10, 10BP10, 20BP10) were attributed to both the dense matrix and the mechanical reinforcement (crack-bridging) provided by the PPF. When the PPF fibers burned at 750°C, the reinforcement effect was eliminated, and the voids they left behind further weakened the matrix. Due to this dual-damage mechanism, these dense blends experienced much greater proportional losses at 750°C than their 28-day strengths (e.g., 51.0% loss for 10BP10; 57.8% loss for 20BP10).

The presence of bentonite significantly improved high-temperature strength, especially in the fiber-free series. The 0BP0 (0% bentonite) mixture lost 27.6% of its 28-day strength at 750°C, while the 20BP0 (20% BC) mixture lost only 5.9%. This demonstrates that bentonite is a highly thermally stable aluminosilicate source. A study by Ebrahim et al. (2024) also reported that geopolymers containing 10% bentonite exhibited the best thermal resistance at 900°C, and bentonite increased thermal stability. Bentonite helps maintain the matrix's structural integrity by forming phases that remain stable or recrystallize (sinter) at high temperatures [24,61].

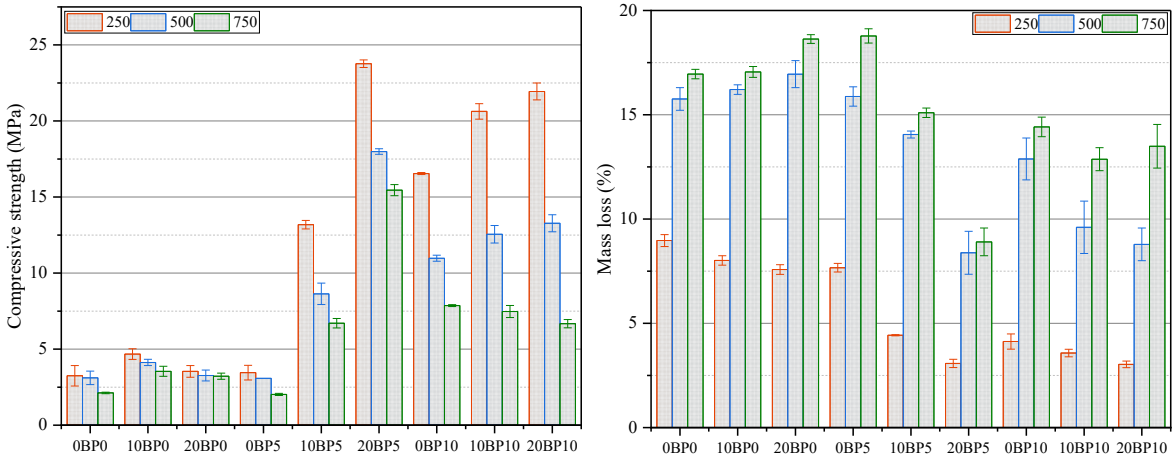

(a) Compressive strength (b) Mass loss

Figure 7. High temperature resistance of GFC samples (Köpük beton numunelerinin yüksek sıcaklık dayanım değerleri)

Mass loss at high temperatures occurs primarily through three mechanisms: (1) evaporation of free and physically bound (adsorbed) water up to 250°C, (2) dehydration of chemically bound water in the geopolymer gel structure and dehydroxylation of bentonite (loss of structural OH) in the range of 400°C-750°C, and (3) melting of PPF (~160-170°C) and loss of mass by combustion at higher temperatures [62–64].

Figure 7b shows the weight losses in GFC samples due to high-temperature effects. Blends 0BP0, 10BP0, 20BP0, and 0BP5, which maintained their stable foam structure (low density, high porosity), exhibited the highest mass losses at all temperature levels. At 750°C, losses in this group ranged from 16.95% to 18.78%. The main reason for this is the high porosity of these mixtures (ranging from 58.6% to 61.2%). The extensive, interconnected pore network not only retains a very high amount of free and physically bound water that can evaporate but also allows heat to penetrate deeply into the material, accelerating dehydration. In the fiber-free (0% PPF) series, as the bentonite content increased (from 0% to 20%), the mass loss at 750°C rose from 16.95 to 18.63. This confirms that bentonite, due to its high water-absorption capacity and layered structure, retains additional (interlayer) water within the matrix, which evaporates at high temperatures, increasing mass loss [65]. This stable foam containing 0.5% PPF showed the highest mass loss of 18.78% at 750°C. This high loss is a combined result of both water evaporation due to high porosity and combustion of 0.5% PPF.

The most remarkable result was that the foam collapsed in the high-density series. Compared with stable foams, these mixtures showed noticeably lower mass loss (8.90% to 15.10% at 750°C). This is because these mixtures are no longer porous foams, as mentioned in earlier analyses. The significant reduction in free water available for evaporation and the macroporous surface area available for water retention due to foam collapse dramatically reduces mass loss at low temperatures (especially 250°C). For example, 0BP5 (stable foam) lost 7.67% of its mass at 250°C, while 20BP5 (slumped mortar) lost only 3.08%. This provides thermal evidence that the two mixtures are microstructurally distinct. As the PPF content increased (from 0.5% to 1.0%), mass loss also increased. For example, the 20BP5 (0.5% PPF) mixture containing 20% bentonite lost 8.90% mass at 750°C, while the 20BP10 (1% PPF) mixture lost 13.49% mass. This is a direct result of the 1% PPF mixture having twice the mass of organic fibers burned as the 0.5% PPF mixture. The 8.90% mass loss of the 20BP5 (20% bentonite, 0.5% PPF) mixture is much lower than the 15.10% loss of the 10BP5 (10% bentonite, 0.5% PPF) mixture. This can be explained by the pozzolanic and sintering behaviour of bentonite, which enhances the matrix's thermal stability at high temperatures. The 20% bentonite helped maintain the integrity of the matrix despite the voids formed by PPF combustion [24].

The relationship between mass loss and samples' compressive strength at high temperatures was analyzed using nonlinear regression; the results are shown in Figure 8. The analysis revealed different correlation patterns depending on the temperature. All temperatures exhibited a significant negative correlation ($R2 > 0.90$). Samples with higher compressive strength lost less weight under all high-

temperature conditions. Conversely, samples with lower compressive strength lost more weight. In high-density samples (like 20BP5), foam collapse created a very dense matrix with very low porosity (around 12%). The limited void space in these samples restricts the amount of free water they can hold, thus increasing the potential for water evaporation and mass loss as temperature rises.

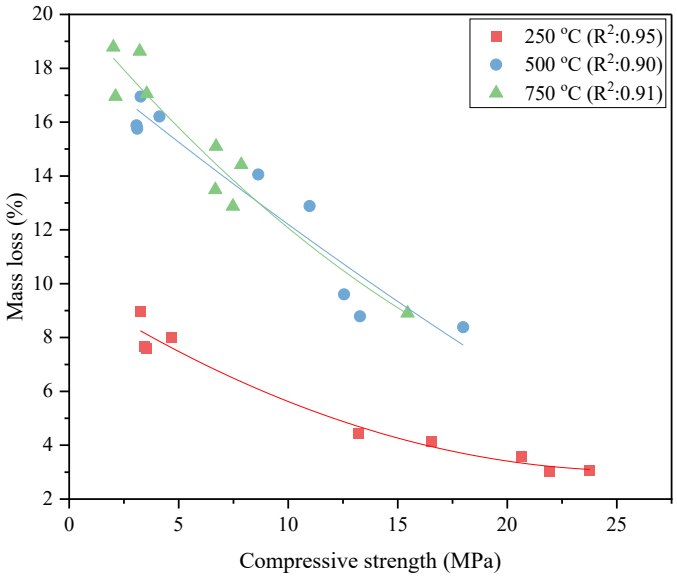

Figure 8. Relationship between compressive strength and mass loss (Kütle kaybı ve basınç dayanımları arasındaki ilişki)

3.6. Freeze-Thaw Resistance (Donma-Çözülme Dayanıklılığı)

Freeze-thaw durability is one of the most significant durability characteristics, particularly for the exterior or structural insulation materials exposed to extreme climatic conditions. Mass loss and compressive strength after 30 F-T cycles showed that the bentonite-PPF composites exhibit significant changes in freeze-damage resistance.

Mass loss is a direct reflection of the scaling and spalling of the material surface resulting from the internal hydraulic pressure generated by the expansion and freezing of water during freeze-thaw cycles. The mixtures exhibiting the most stable foam structure (0BP0, 10BP0, 20BP0, and 0BP5) showed the most significant mass losses, ranging from 3.03% to 3.33% (Figure 9). This is a natural consequence of high apparent porosity (58.6% to 61.2%) and high water absorption (43.6% to 50.4%) in previous analyses. An extensive network of open macropores allowed deep water intrusion into the material (high capillarity). Freezing of pore water produced high internal stresses, leading to matrix fragmentation and mass loss [66].

All the other mixes (10BP5, 20BP5, 0BP10, 10BP10, 20BP10) with foam collapse and transformed into a dense mortar texture exhibited much lower mass loss, ranging from 1.84% to 2.81%. The superiority of this group in F-T strength stems from the dense microstructure resulting from foam collapse. These blends' low porosity (11.9% versus 21.7%) and low water absorption capacity (7.2% versus 12.7%) suppressed water penetration into the matrix, thereby reducing freeze-thaw damage. The lowest mass loss (1.84%) was observed with the 20BP5 mix, which had the highest hardened density (1779 kg/m^3) and the lowest porosity (11.9%). Comparison with its stable foam counterpart, 0BP5 (3.33% loss), shows that foam deflation-induced densification increased freeze-thaw resistance (mass loss) by 44.7%.

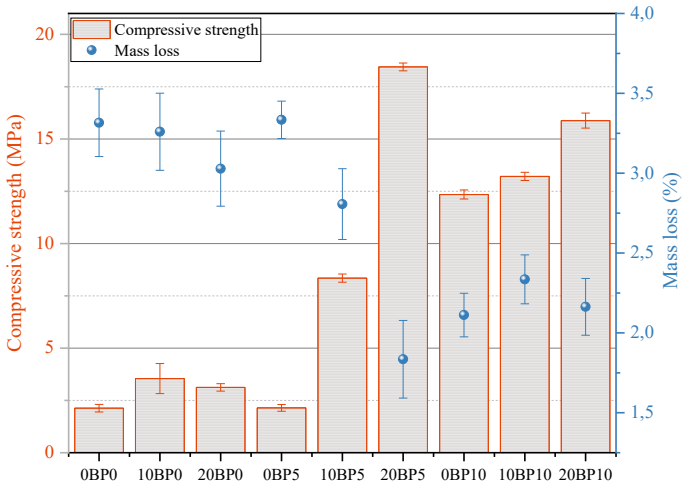

Figure 9. Mechanical and physical properties of F-T cycled GFCs (Köpük betonların donma-çözülme etkisi altında mekanik ve fiziksel özellikleri)

The series of high-mass-loss stable foams (0BP0, 10BP0, 20BP0, and 0BP5) had low absolute residual strengths ranging from 2.13 MPa to 3.55 MPa (Figure 8). This indicates that freeze-thaw cycles further weakened the internal bonds of the already mechanically weak porous structure. Of special mention among this group is bentonite's protective role. 10BP0 (10% bentonite) mixture possessed a 66.7% improvement of post-F-T strength compared with the control 0BP0 (0% bentonite, 2.13 MPa), and its residual strength was 3.55 MPa. This is an even larger percentage improvement than for 28-day strength (approximately 30%). This suggests that bentonite not only strengthens pore walls through pozzolanic reactions but also improves the matrix microstructure (pore refinement), making it more resistant to freeze-thaw cycles [44].

The foam-densified mortars by collapse exhibited extremely high residual compressive strengths ranging from 8.35 MPa to 18.45 MPa. These are incredibly high-strength values attained by these materials after being almost imperceptibly impaired by F-T cycles. The highest residual strength of 18.45 MPa was achieved by the 20BP5 mixture, which exhibited the least mass loss of 1.84%. This is 766% higher than that of the stable foam control sample 0BP0 (2.13 MPa). The effects of PPF and bentonite are also evident in this dense mortar series. In the 1% PPF series, 20BP10 (20% BC) was 15.88 MPa (28.7% improvement), whereas 0BP10 (0% bentonite) achieved 12.34 MPa. This indicates that bentonite also enhances the freeze-thaw resistance of the dense matrix. The PPF fibers, on the other hand, provide second-level protection by preventing the spread of microcracks formed by freeze-thaw cycles within this high-density matrix through "crack-bridging" [67].

3.7. Microstructure (Mikroyapı)

Figure 10a shows the microstructure of the reference mixture (0BP0), which contains no additives (bentonite or fiber). As expected, the matrix displays a morphology dominated by calcium aluminosilicate hydrate (C-A-S-H) gels resulting from GBFS alkali activation. However, the widespread 'hairline cracks,' indicated by the arrows, reveal the matrix's susceptibility to drying shrinkage and poor structural integrity. This extensive network of microcracks and a loose gel texture provides microstructural evidence for why sample 0BP0 has some of the lowest mechanical performance levels in the series (2.94 MPa).

The 10BP5 mixture, which contains 10% bentonite and 0.5% fiber (see Figure 10b), visually confirms the 'stable foam' structure—the most critical finding of the study. The intact spherical air bubble, clearly visible in the image, proves that the rheological threshold was not exceeded in this mixture and that the foam stayed trapped within the matrix without collapsing. This explains the sample's low density (lightness) and high insulation performance (0.172 W/m.K). Additionally, the addition of bentonite produced denser, more amorphous sodium aluminosilicate hydrate (N-A-S-H) gels within the matrix. These gels then formed a hybrid structure with the C-A-S-H network.

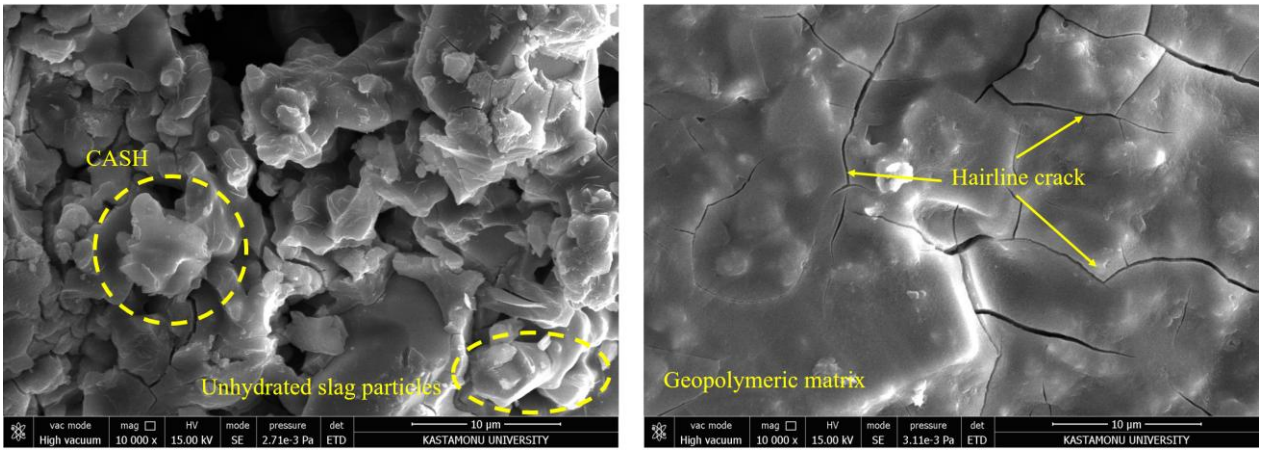

(a) 0BP0 mixture

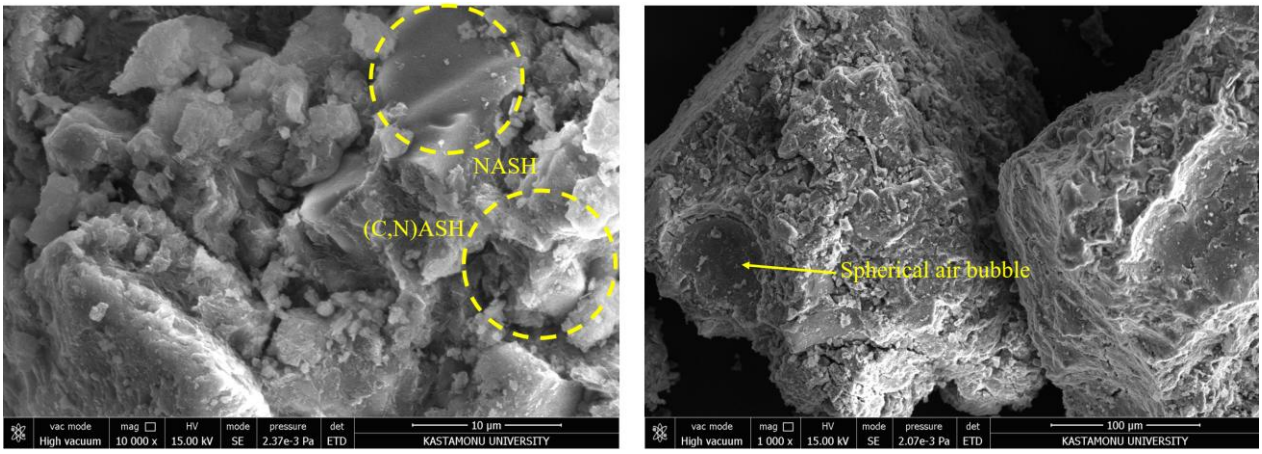

(b) 10BP5 mixture

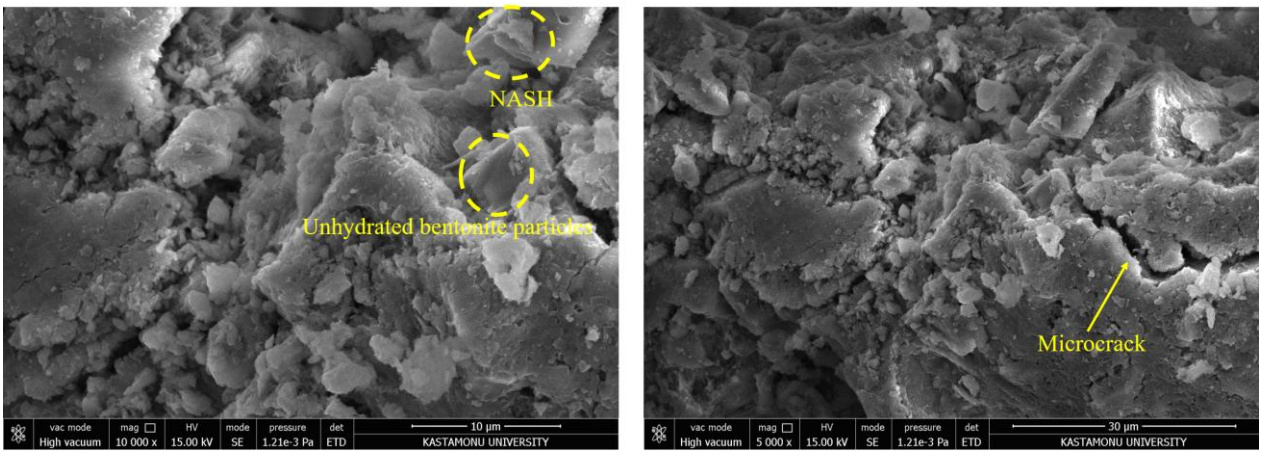

(c) 20BP10 mixture

Figure 10. Microstructure images of GFC mixtures (Köpük beton numunelerine ait mikroyapı görüntüleri)

Figure 10c shows the highly dense structure formed by the 20BP10 mixture containing 20% bentonite and 1% PPF after 'foam extinguishing.' The spherical air voids seen in Figure (b) have completely vanished here, replaced by a compact block where C-A-S-H and bentonite-derived N-A-S-H gels are intertwined. Although the 'microcracks' observed within the matrix suggest high rigidity, the overall integrity remains intact. Additionally, angular particles (unreacted

slag/bentonite) embedded in the gel phase that have not fully dissolved have created a micro-filler effect, supporting the skeletal structure. This dense, void-free morphology explains why the sample achieves a high density of 1779 kg/m³ and superior strength around ~18-20 MPa.

In summary, microstructural evidence clearly influences the macroscopic behaviour of composites. For stable foam mixes, such as 10BP5, maintaining the intact spherical macro-pore network results in a reduction of structural strength (~2-3 MPa), but it correlates with high apparent porosity (61.2%), low fresh and hardened densities (~640 kg/m³), and excellent thermal insulation (0.172 W/m.K). Conversely, the “foam collapse” mechanism observed in high-dose mixes such as 20BP10 significantly alters macro-behaviour. The disappearance of air voids and the presence of unreacted micro-fillers alongside C-A-S-H and N-A-S-H gels—factors that densify the matrix—directly lead to decreased porosity (11.9%), increased density (1779 kg/m³), higher pressure resistance (~18-20 MPa), and a substantial improvement in freeze-thaw durability. Ultimately, the microstructural phase transition driven by rheological factors is the key determinant of these materials' physical, thermal, and mechanical properties.

The macroscopic results, especially the notable increases in bending and compressive strength, indirectly suggest that the polypropylene fibers are evenly distributed and effectively bridge cracks. However, the current SEM images did not capture direct microstructural details of the fiber-matrix interface (ITZ) or fiber pull-out mechanisms. Poor fiber distribution, such as clumping, usually causes significant strength reductions, so the consistent mechanical improvements in this study indicate good fiber-matrix bonding. Nonetheless, future high-resolution micromechanical imaging focused on the fiber-matrix interface will be essential to visually confirm these macro-level observations.

4. CONCLUSIONS (SONUÇLAR)

In this study, the fresh, physical, mechanical, and durability properties of polypropylene fiber (PPF)-reinforced geopolymer foam concretes (GFCs) containing Blast Furnace Slag (GBFS) and partial bentonite replacement, activated with a one-part alkali activator (powdered sodium metasilicate), were investigated. Based on the experimental results, the following main conclusions were reached:

a) The most important discovery is that exceeding a certain threshold of additives (PPF >0.5% or bentonite >10% with fibers) disrupts the rheology of fresh mortar. Higher viscosity and internal friction cause stable foam bubbles to break down mechanically during mixing, transforming the material from lightweight foam into dense mortar.

b) This rheological change leads to a notable difference in material performance. Stable foams offer excellent thermal insulation (0.172 W/m·K), but they have low mechanical strength. In contrast, "collapsed" dense mortars demonstrate exceptional compressive strength (>20 MPa) and high structural integrity. However, they lose their insulating properties and become thermally conductive (0.543 W/m·K).

c) Microstructural densification caused by foam collapse significantly enhances durability. While stable porous foams experienced high mass loss during freeze-thaw cycles, dense mortars demonstrated better resistance (mass loss of less than 2%) and maintained high residual strength. Additionally, bentonite was identified as a crucial additive for thermal stability, reducing strength loss at high temperatures (750°C).

d) To create lightweight, insulating GFCs that do not collapse, the mix must stay within a 'safe window'. The PPF content should be no more than 0.5%, and the bentonite replacement should be less than 10%.

e) This study quantitatively analyzed the macroscopic pore structure changes using apparent porosity and sorptivity tests. However, it did not include advanced microstructural analysis methods like Mercury Intrusion Porosimetry or X-ray Micro-CT. Future research using these techniques to precisely measure pore-size distribution and track how the matrix topology evolves during 'foam collapse' will offer a more detailed understanding of this process..

DECLARATION OF ETHICAL STANDARDS (ETİK STANDARTLARIN BEYANI)

The author of this article declares that the materials and methods they use in their work do not require ethical committee approval and/or legal-specific permission.

Bu makalenin yazarı çalışmalarında kullandıkları materyal ve yöntemlerin etik kurul izni ve/veya yasal-özel bir izin gerektirmediğini beyan ederler.

AUTHORS' CONTRIBUTIONS (YAZARLARIN KATKILARI)

***Oğuzhan Yavuz BAYRAKTAR*:** He conducted the experiments, analyzed the results and performed the writing process.

Deneyleri yapmış, sonuçlarını analiz etmiş ve maklenin yazım işlemini gerçekleştirmiştir.

***Gökhan KAPLAN*:** He conducted the experiments, analyzed the results and performed the writing process.

Deneyleri yapmış, sonuçlarını analiz etmiş ve maklenin yazım işlemini gerçekleştirmiştir.

CONFLICT OF INTEREST (ÇIKAR ÇATIŞMASI)

There is no conflict of interest in this study.

Bu çalışmada herhangi bir çıkar çatışması yoktur.

REFERENCES (KAYNAKLAR)

[1] A. Mohsen, M.S. Amin, M. Ramadan, Synthesis of highly efficient microwaved geopolymer based on alkaline activation of slag/bentonite precursors: The correlation among hydraulic phases, porosity profile, and compressive strength, Constr. Build. Mater. 476 (2025) 141299. https://doi.org/10.1016/j.conbuildmat.2025.141299.

[2] S. Sbahieh, G. McKay, A. Nurdiawati, S.G. Al-Ghamdi, The sustainability of partial and total replacement of Ordinary Portland Cement: A deep dive into different concrete mixtures through life cycle assessment, J. Build. Eng. 108 (2025) 112830. https://doi.org/10.1016/j.jobe.2025.112830.

[3] M.U. Yılmazoğlu, İ. Türkel, B. Bayrak, İ.G. Mütevelli Özkan, E. Kulaoğlu, O.Y. Bayraktar, K. Toklu, G. Kaplan, Green prepacked foam concretes against environmental attacks: The role of waste aluminum shavings, cooling methods and binder modifications, J. Build. Eng. 114 (2025) 114232. https://doi.org/10.1016/j.jobe.2025.114232.

[4] H. Nasreddine, N. Dujardin, A. Djerbi, T. Salem, L. Gautron, Impact of hemp shiv content and binder type on the thermal and mechanical properties of geopolymer composites, Constr. Build. Mater. 476 (2025) 141297. https://doi.org/10.1016/j.conbuildmat.2025.141297.

[5] G. Zhang, K. Li, H. Shi, C. Chen, C. Yuan, Study on the Effects and Mechanisms of Fly Ash, Silica Fume, and Metakaolin on the Properties of Slag–Yellow River Sediment-Based Geopolymers, Materials 18 (2025) 1845. https://doi.org/10.3390/ma18081845.

[6] Y. Fu, X. Wang, L. Wang, Y. Li, Foam concrete: a state-of-the-art and state-of-the-practice review, Adv. Mater. Sci. Eng. 2020 (2020) 6153602.

[7] Z. Zhang, J.L. Provis, A. Reid, H. Wang, Mechanical, thermal insulation, thermal resistance and acoustic absorption properties of geopolymer foam concrete, Cem. Concr. Compos. 62 (2015) 97–105. https://doi.org/10.1016/j.cemconcomp.2015.03.013.

[8] J.S. Narayanan, K. Ramamurthy, Identification of set-accelerator for enhancing the productivity of foam concrete block manufacture, Constr. Build. Mater. 37 (2012) 144–152.

[9] M. Abdellatief, A.E. Hassanien, M. Mortagi, H. Hamouda, Geopolymer foam concrete: a review of pore characteristics, compressive strength and artificial intelligence in GFC strength simulations, Discov. Concr. Cem. 1 (2025) 4. https://doi.org/10.1007/s44416-025-00003-x.

[10] İ. Türkel, M.U. Yilmazoğlu, İ.G.M. Özkan, O.Y. Bayraktar, G. Kaplan, Production of Environmentally Friendly Foam Concrete Using Waste Material: Effects of Waste Concrete Sludge and Fiber Additives, Gazi Üniversitesi Fen Bilim. Derg. Part C Tasar. Ve Teknol. 13 (2025) 1384–1395. https://doi.org/10.29109/gujsc.1612287.

[11] M. Khan, M. Shakeel, K. Khan, S. Akbar, A. Khan, A Review on Fiber-Reinforced Foam Concrete, Eng. Proc. 22 (2022) 13. https://doi.org/10.3390/engproc2022022013.

[12] K. Dhasindrakrishna, S. Ramakrishnan, K. Pasupathy, J. Sanjayan, Collapse of fresh foam concrete: Mechanisms and influencing parameters, Cem. Concr. Compos. 122 (2021) 104151. https://doi.org/10.1016/j.cemconcomp.2021.104151.

[13] H. Yue, Z. Zhang, S. Hua, Y. Gao, S. Cui, Y. Wang, Z. Zhang, H. Zhu, Solid waste-based set-on-demand 3D printed concrete: Active rheological control of cement-based magneto-rheological fluids, Constr. Build. Mater. 404 (2023) 133269. https://doi.org/10.1016/j.conbuildmat.2023.133269.

[14] C. Liu, X. Wang, Y. Chen, C. Zhang, L. Ma, Z. Deng, C. Chen, Y. Zhang, J. Pan, N. Banthia, Influence of hydroxypropyl methylcellulose and silica fume on stability, rheological properties, and printability of 3D printing foam concrete, Cem. Concr. Compos. 122 (2021)

104158. https://doi.org/10.1016/j.cemconcomp.2021.104158.

[15] J.M. Beltrán, L. Chica, On fresh state behavior of foamed cement pastes and its influence on hardened performance, Constr. Build. Mater. 368 (2023) 130518. https://doi.org/10.1016/j.conbuildmat.2023.130518.

[16] A. Ahıskalı, B. Bayrak, K. Toklu, O.Y. Bayraktar, G. Kaplan, A.C. Aydın, Characterizing the Chemistry of One-Part Green Geopolymer Foams: The Role of Silica Fume and Fiber Hybridization, ACS Omega 10 (2025) 20193–20212.

[17] A. Öz, F.M. Dursun, A. Benli, G. Kaplan, Optimization of sustainable high-performance alkali-activated composites using industrial and agricultural wastes: A comprehensive performance evaluation, J. Build. Eng. (2025) 113319.

[18] M. Amran, S. Debbarma, T. Ozbakkaloglu, Fly ash-based eco-friendly geopolymer concrete: A critical review of the long-term durability properties, Constr. Build. Mater. 270 (2021) 121857.

[19] Y.N. Wibowo, B. Piscesa, Y. Tajunnisa, W. Sutrisno, Investigation on the mechanical behavior of high-calcium fly ash geopolymer concrete using one-part method, Constr. Build. Mater. 490 (2025) 142436. https://doi.org/10.1016/j.conbuildmat.2025.142436.

[20] S. Jahandari, Z. Tao, A. Rahmani, M.A. Alim, Durability of one-part geopolymer concrete in aggressive environments, Constr. Build. Mater. 490 (2025) 142510.

[21] R.M. Waqas, S. Zaman, M.K. Alkharisi, F. Butt, E. Alsuhaibani, Influence of Bentonite and Polypropylene Fibers on Geopolymer Concrete, Sustainability 16 (2024) 789. https://doi.org/10.3390/su16020789.

[22] S.A. Memon, R. Arsalan, S. Khan, T.Y. Lo, Utilization of Pakistani bentonite as partial replacement of cement in concrete, Constr. Build. Mater. 30 (2012) 237–242. https://doi.org/10.1016/j.conbuildmat.2011.11.021.

[23] B. Masood, A. Elahi, S. Barbhuiya, B. Ali, Mechanical and durability performance of recycled aggregate concrete incorporating low calcium bentonite, Constr. Build. Mater. 237 (2020) 117760. https://doi.org/10.1016/j.conbuildmat.2019.117760.

[24] A. allah M. Ebrahim, D.A. Ahmed, R. Abu-Elwafa, Development of an eco-friendly geopolymer mortar using slag and fly ash with high bentonite content for thermal and environmental applications, Sci. Rep. 14 (2024) 26727. https://doi.org/10.1038/s41598-024-76780-5.

[25] C. Chen, S. Cheng, X. Yu, J. Song, Y. Huang, Y. Jiang, Research on the mechanical properties and durability of polypropylene fiber-reinforced ultra-fine iron tailings sand foam concrete, Constr. Build. Mater. 495 (2025) 143734.

[26] J. Ríos, H. Cifuentes, C. Leiva, M. Ariza, M. Ortiz, Effect of polypropylene fibers on the fracture behavior of heated ultra-high performance concrete, Int. J. Fract. 223 (2020) 173–187.

[27] Z.F. Akbulut, E. Kuzielová, T.A. Tawfik, P. Smarzewski, S. Guler, Synergistic effects of polypropylene fibers and silica fume on structural lightweight concrete: analysis of workability, thermal conductivity, and strength properties, Materials 17 (2024) 5042.

[28] E. Silva, J. Coelho, J. Bordado, Strength improvement of mortar composites reinforced with newly hybrid-blended fibres: Influence of fibres geometry and morphology, Constr. Build. Mater. 40 (2013) 473–480.

[29] A.K.F. Gaddafi, U.J. Alengaram, N.M. Bunnori, S.I. Muhammad, S. Ibrahim, M. Sumesh, Mechanical properties, flexural behaviour, and ductility characteristics of fibre-reinforced geopolymer mortar, Constr. Build. Mater. 403 (2023) 133109.

[30] A. Achour, F. Ghomari, N. Belayachi, Properties of cementitious mortars reinforced with natural fibers, J. Adhes. Sci. Technol. 31 (2017) 1938–1962.

[31] J. Sun, Y. Guo, Y. Meng, R. Jia, J. Zhou, H. Gao, J. Liu, Effects of silicate modulus and GBFS content on shrinkage of alkali-activated steel slag cementitious material, J. CO2 Util. 91 (2025) 103015.

[32] T.A. Fode, Y.A.C. Jande, T. Kivevele, Activated bentonite for physical, mechanical, and durability properties of concrete—a review, Adv. Civ. Eng. 2024 (2024) 3849110.

[33] M.O. Ghone, G. Long, K. Yang, X. Ma, N. Islam, Toughness improvement of low strength ceramsite lightweight concrete by polypropylene fiber and recycled rubber particle, Constr. Build. Mater. 422 (2024) 135716.

[34] A. Ahıskalı, M. Ahıskalı, O.Y. Bayraktar, G. Kaplan, J. Assaad, Mechanical and durability properties of polymer fiber reinforced one-part foam geopolymer concrete: A sustainable strategy for the recycling of waste

steel slag aggregate and fly ash, Constr. Build. Mater. 440 (2024) 137492.

[35] J. Junior, A.K. Saha, P.K. Sarker, A. Pramanik, Workability and Flexural Properties of Fibre-Reinforced Geopolymer Using Different Mono and Hybrid Fibres, Materials 14 (2021) 4447. https://doi.org/10.3390/ma14164447.

[36] O. Gencel, M. Nodehi, O. Yavuz Bayraktar, G. Kaplan, A. Benli, A. Gholampour, T. Ozbakkaloglu, Basalt fiber-reinforced foam concrete containing silica fume: An experimental study, Constr. Build. Mater. 326 (2022) 126861. https://doi.org/10.1016/j.conbuildmat.2022.126861.

[37] E.K.K. Nambiar, K. Ramamurthy, Models relating mixture composition to the density and strength of foam concrete using response surface methodology, Cem. Concr. Compos. 28 (2006) 752–760. https://doi.org/10.1016/j.cemconcomp.2006.06.001.

[38] Q. Song, Y. Zou, P. Zhang, S. Xu, Y. Yang, J. Bao, S. Xue, J. Liu, S. Gao, L. Lin, Novel high-efficiency solid particle foam stabilizer: Effects of modified fly ash on foam properties and foam concrete, Cem. Concr. Compos. 155 (2025) 105818. https://doi.org/10.1016/j.cemconcomp.2024.105818.

[39] A. Ahıskalı, A. Benli, M. Ahıskalı, O.Y. Bayraktar, G. Kaplan, Sustainable geopolymer foam concrete with recycled crumb rubber and dual fiber reinforcement of polypropylene and glass fibers: A comprehensive study, Constr. Build. Mater. 474 (2025) 141137. https://doi.org/10.1016/j.conbuildmat.2025.141137.

[40] Y. Fu, X. Wang, L. Wang, Y. Li, Foam Concrete: A State-of-the-Art and State-of-the-Practice Review, Adv. Mater. Sci. Eng. 2020 (2020) 6153602. https://doi.org/10.1155/2020/6153602.

[41] G. Zhou, R.K.L. Su, A Review on Durability of Foam Concrete, Buildings 13 (2023) 1880. https://doi.org/10.3390/buildings13071880.

[42] A. Raj, D. Sathyan, K.M. Mini, Physical and functional characteristics of foam concrete: A review, Constr. Build. Mater. 221 (2019) 787–799. https://doi.org/10.1016/j.conbuildmat.2019.06.052.

[43] T. Liu, Y. Zhong, Z. Han, W. Xu, Deformation characteristics and countermeasures for a tunnel in difficult geological environment in NW China, Adv. Civ. Eng. 2020 (2020) 1694821.

[44] R.M. Waqas, S. Zaman, M.K. Alkharisi, F. Butt, E. Alsuhaibani, Influence of Bentonite and Polypropylene Fibers on Geopolymer Concrete, Sustainability 16 (2024) 789. https://doi.org/10.3390/su16020789.

[45] C.S. Das, T. Dey, R. Dandapat, B.B. Mukharjee, J. Kumar, Performance evaluation of polypropylene fibre reinforced recycled aggregate concrete, Constr. Build. Mater. 189 (2018) 649–659. https://doi.org/10.1016/j.conbuildmat.2018.09.036.

[46] Z. Zhang, J.L. Provis, A. Reid, H. Wang, Geopolymer foam concrete: An emerging material for sustainable construction, Constr. Build. Mater. 56 (2014) 113–127. https://doi.org/10.1016/j.conbuildmat.2014.01.081.

[47] A.M. Aragoncillo, D. Cleary, U. Thayasivam, G. Lomboy, Water sorptivity prediction model for concrete with all coarse recycled concrete aggregates, Constr. Build. Mater. 394 (2023) 132128. https://doi.org/10.1016/j.conbuildmat.2023.132128.

[48] C.K. Yip, G.C. Lukey, J.S.J. van Deventer, The coexistence of geopolymeric gel and calcium silicate hydrate at the early stage of alkaline activation, Cem. Concr. Res. 35 (2005) 1688–1697. https://doi.org/10.1016/j.cemconres.2004.10.042.

[49] A. Sharmin, U.J. Alengaram, M.Z. Jumaat, M.O. Yusuf, S.M.A. Kabir, I.I. Bashar, Influence of source materials and the role of oxide composition on the performance of ternary blended sustainable geopolymer mortar, Constr. Build. Mater. 144 (2017) 608–623. https://doi.org/10.1016/j.conbuildmat.2017.03.178.

[50] R. Porkodi, S. Dharmar, S. Nagan, Experimental study on fiber reinforced Self-compacting geopolymer mortar, Int. J. Adv. Res. Sci. Eng. 4 (2015) 968–977.

[51] Z.A. Mohammed, L.A. Al-Jaberi, A.N. Shubber, Effect of polypropylene fiber on properties of geopolymer concrete based metakolin, J. Eng. Sustain. Dev. 25 (2021) 58–67.

[52] H. Awang, M.H. Ahmad, Durability properties of foamed concrete with fiber inclusion, Int. J. Civ. Struct. Constr. Archit. Eng. 8 (2014) 273–276.

[53] Y. Liu, L. Wang, K. Cao, L. Sun, Review on the Durability of Polypropylene Fibre-

Reinforced Concrete, Adv. Civ. Eng. 2021 (2021) 6652077. https://doi.org/10.1155/2021/6652077.

[54] M. Chen, D. Wu, K. Chen, C. Liu, G. Zhou, P. Cheng, The effects of solid activator dosage and the liquid-solid ratio on the properties of FA-GGBS based one-part geopolymer, Constr. Build. Mater. 463 (2025) 140067. https://doi.org/10.1016/j.conbuildmat.2025.140067.

[55] J. Zeng, K. Zhang, W. Sun, Y. Zeng, Z. Zou, Mechanics and microstructure analysis of geopolymer utilizing ilmenite tailing and metakaolin powder as alkali-activated materials, Case Stud. Constr. Mater. 21 (2024) e03567. https://doi.org/10.1016/j.cscm.2024.e03567.

[56] H. Li, X. Hu, D. Zhu, C. Shi, Effects of oxide compositions of vitreous phases in precursors on the chloride binding of geopolymer, Cem. Concr. Compos. 165 (2026) 106357. https://doi.org/10.1016/j.cemconcomp.2025.106357.

[57] M. Jones, A. McCarthy, Behaviour and assessment of foamed concrete for construction applications, in: Thomas Telford Publishing, 2005: pp. 61–88.

[58] Q. Song, Y. Zou, P. Zhang, S. Xu, Y. Yang, J. Bao, S. Xue, J. Liu, S. Gao, L. Lin, Novel high-efficiency solid particle foam stabilizer: Effects of modified fly ash on foam properties and foam concrete, Cem. Concr. Compos. 155 (2025) 105818.

[59] A. Öz, A.S. Jamal, B. Bayrak, X. Song, G. Kaplan, A.C. Aydın, Effect of apricot kernel ash on the performance of sustainable alkali-activated composites, Mater. Chem. Phys. 339 (2025) 130748.

[60] J. Shi, B. Liu, S.H. Chu, Y. Zhang, Z. Zhang, K. Han, Recycling air-cooled blast furnace slag in fiber reinforced alkali-activated mortar, Powder Technol. 407 (2022) 117686. https://doi.org/10.1016/j.powtec.2022.11768

[61] D. Ahmed, E. Kishar, Effect of elevated temperatures on the performance of metakaolin geopolymer pastes incorporated by cement kiln dust, Egypt. J. Chem. 64 (2021) 1911–1926.

[62] M.S. Morsy, A.M. Rashad, H. Shoukry, M.M. Mokhtar, Potential use of limestone in metakaolin-based geopolymer activated with H3PO4 for thermal insulation, Constr. Build. Mater. 229 (2019) 117088. https://doi.org/10.1016/j.conbuildmat.2019.117088.

[63] M. Önal, Y. Sarıkaya, Thermal behavior of a bentonite, J. Therm. Anal. Calorim. 90 (2007) 167–172. https://doi.org/10.1007/s10973-005-7799-9.

[64] H. Wu, X. Lin, A. Zhou, A review of mechanical properties of fibre reinforced concrete at elevated temperatures, Cem. Concr. Res. 135 (2020) 106117. https://doi.org/10.1016/j.cemconres.2020.106117.

[65] V. Zivica, M.T. Palou, Physico-chemical characterization of thermally treated bentonite, Compos. Part B Eng. 68 (2015) 436–445. https://doi.org/10.1016/j.compositesb.2014.07.019.

[66] V. Kočí, R. Černý, Directly foamed geopolymers: A review of recent studies, Cem. Concr. Compos. 130 (2022) 104530. https://doi.org/10.1016/j.cemconcomp.2022.104530.

[67] W.D.A. Rickard, L. Vickers, A. van Riessen, Performance of fibre reinforced, low density metakaolin geopolymers under simulated fire conditions, Appl. Clay Sci. 73 (2013) 71–77. https://doi.org/10.1016/j.clay.2012.10.006.